

**PERFORMANCE ANALYSIS OF SUCRe PROTOCOL
USING SOFT DECISION RULE**

A DISSERTATION

*Submitted in partial fulfilment of the
requirements for the award of the degree of*

MASTER OF TECHNOLOGY

in

ELECTRONICS AND COMMUNICATION ENGINEERING

(With Specialization in Communication Systems)

By

AAKANKSHA GUPTA

(Enrolment No. 17531001)

Under the guidance of

DR. MEENAKSHI RAWAT



DEPARTMENT OF ELECTRONICS AND COMMUNICATION ENGINEERING
INDIAN INSTITUTE OF TECHNOLOGY, ROORKEE

ROORKEE-247667 (INDIA)

JUNE 2019

CANDIDATE’S DECLARATION

I hereby declare that the work presented in this dissertation report entitled “**PERFORMANCE ANALYSIS OF SUCRe PROTOCOL USING SOFT DECISION RULE**” towards the partial fulfilment of the requirements for the award of the degree of **MASTER OF TECHNOLOGY** with specialization in **Communication Systems**, submitted in the Department of Electronics and Communication Engineering, Indian Institute of Technology Roorkee, Roorkee (India) is an authentic record of my own work carried out during the period from July 2018 to May 2019, under the guidance and supervision of **Dr. Meenakshi Rawat**, Assistant Professor, Department of Electronics and Communication Engineering, Indian Institute of Technology Roorkee, Roorkee (India).

The matter presented in this dissertation has not been submitted by me for the award of any other degree of this or any other institution.

Date:

Place: Roorkee

(Aakanksha Gupta)

Enrolment No.:17531001

ECE Department

IIT Roorkee

CERTIFICATE

This is to certify that the above statement made by the candidate is correct to the best of my knowledge and belief.

Date:

Place: Roorkee

(Dr. Meenakshi Rawat)

Assistant Professor

ECE Department

IIT Roorkee

ACKNOWLEDGEMENT

I take this opportunity to express my profound gratitude to **Dr. Meenakshi Rawat** (Asst. Prof., ECE Dept., IIT Roorkee) whose exemplary guidance and continued support was a source of inspiration for me throughout the course of this work.

I would also like to thank almighty and my parents for their constant encouragement.



(Aakanksha Gupta)

Enrolment No. 17531001

ECE Department

IIT Roorkee

ABSTRACT

The massive multiple-input multiple-output (MIMO) has great potential to manage fast growth of wireless data traffic. As the number of user equipment (UEs) increases, while each UE intermittently accesses the network, the random access functionality becomes essential as the number of pilots remains very limited. This dissertation work focuses on random access problem in massive MIMO context. A re-engineered protocol named *Strongest User Collision Resolution (SUCRe)* has been developed and its performance has been verified over different fading scenarios starting from the basic Rayleigh to more realistic channels like eta-mu and kappa-mu channels.

In a crowded urban scenario where more than one UEs will be contending for the same pilot, access will be given to UE with the strongest signal at the receiver. The simulations which are done on MATLAB 2018b show that this protocol resolves the majority of pilot collisions occurring in the crowded urban scenario and continues to admit UEs efficiently in overloaded networks.

Once its collision resolution capability has been verified on a simple fading case, its performance is tested on other more realistic channels (Rician, Hoyt, Nakagami-m, eta-mu, kappa-mu, and alpha-mu channels) and the comparative analysis is done.

Contents

Acknowledgement	i
Abstract	ii
List of figures	v
List of tables	vii
Abbreviations	viii
Symbols	ix
1. Introduction	1
1.1 Motivation.....	1
1.2 Massive MIMO systems.....	2
1.3 Channel hardening and favourable propagation properties.....	2
1.3.1 channel hardening.....	2
1.3.2 Favourable propagation.....	3
2. Random access protocol in massive MIMO systems	4
2.1 Classification of collision resolution techniques.....	4
2.2 Random access functionality in LTE.....	5
2.3 Random access functionality in massive MIMO.....	6
3. Conventional SUCR (strongest user collision resolution) protocol	8
3.1 General considerations.....	8
3.2 SUCRe overview.....	9
3.3 System model of SUCRe.....	11
4. Retransmission based on “soft decision rule”	17

4.1 Proposed “soft decision rule”17

5. performance evaluation and numerical results.....20

 5.1 Simulation setup.....20

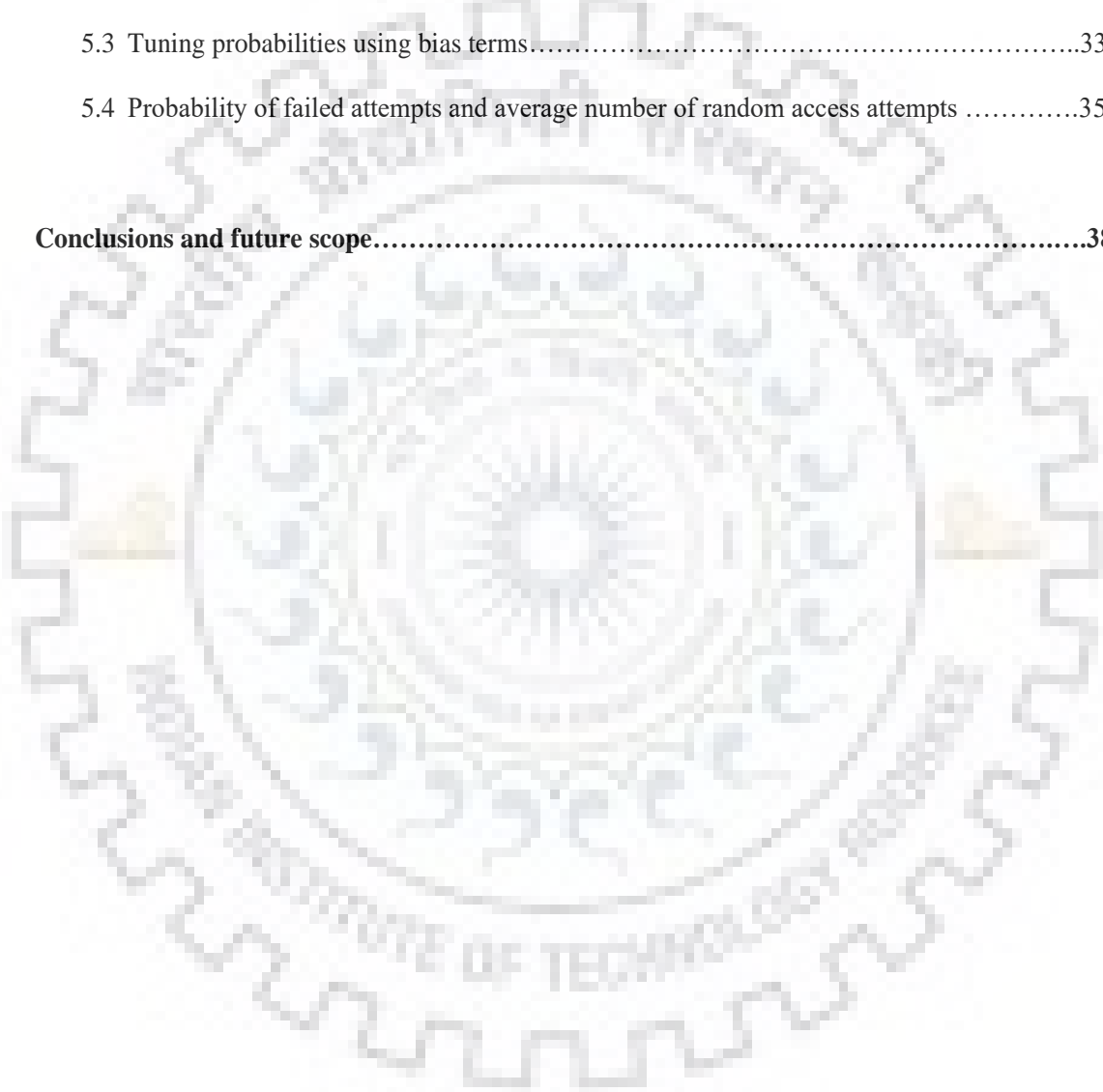
 5.1.1 Channel propagation models.....20

 5.2 The probability to resolving collisions by SUCRe protocol.....30

 5.3 Tuning probabilities using bias terms.....33

 5.4 Probability of failed attempts and average number of random access attempts35

6. Conclusions and future scope.....38



List of Figures


	Page no.
1. The basic massive MIMO transmission	2
2. Random access to pilots (RAP)	5
3. PRACH protocol used in LTE	6
4. Division of time-frequency domain into coherence intervals in SUCRe protocol	9
5. Conventional SUCRe protocol	9
6. Retransmission of the strongest UE is done in the third step	10
7. Probability of retransmission based on the conventional hard decision and the proposed “ <i>soft decision rule</i> ”	18
8. SUCRe protocol performance over Hoyt fading channel for different values of q	22
9. SUCRe protocol performance over the rician fading channel with different Rician factors	23
10. SUCRe protocol performance over Nakagami- m channels for different values of fading parameter m	25
11. SUCRe protocol performance over the η - μ channel for different value of η and μ	27
12. SUCRe protocol performance over the κ - μ channel for different value of κ and μ	28
13. SUCRe protocol performance over the α - μ channel for different value of α and μ	30
14. Probability of resolving collisions, as a function of the number of BS antennas, in a highly loaded cellular network with or without inter-cell interference	32
15. For different bias terms in the hard decision rule, the probability of resolving collisions, false negatives and false positives are illustrated.	35
16. RA performance in a crowded urban scenario. (a) The average number of RA attempts for SUCRe and soft SUCRe. (b) Probability of failed attempts	37
17. Average number of pilot retransmission	38

List of Tables

	Page no.
1. Difference between PRACH and SUCRe protocol	10
2. Different fading channels and their properties	31
3. Simulation parameters for the evaluation of the probability of resolving collisions	32
4. Comparison of SUCRe protocol over different fading channels	34
5. Simulation parameters for the evaluation of the average number of access attempts and the probability of failed attempts	36
6. Reduction in the average number of RA attempts and increment of active UEs in soft SUCRe in comparison with conventional SUCRe	37

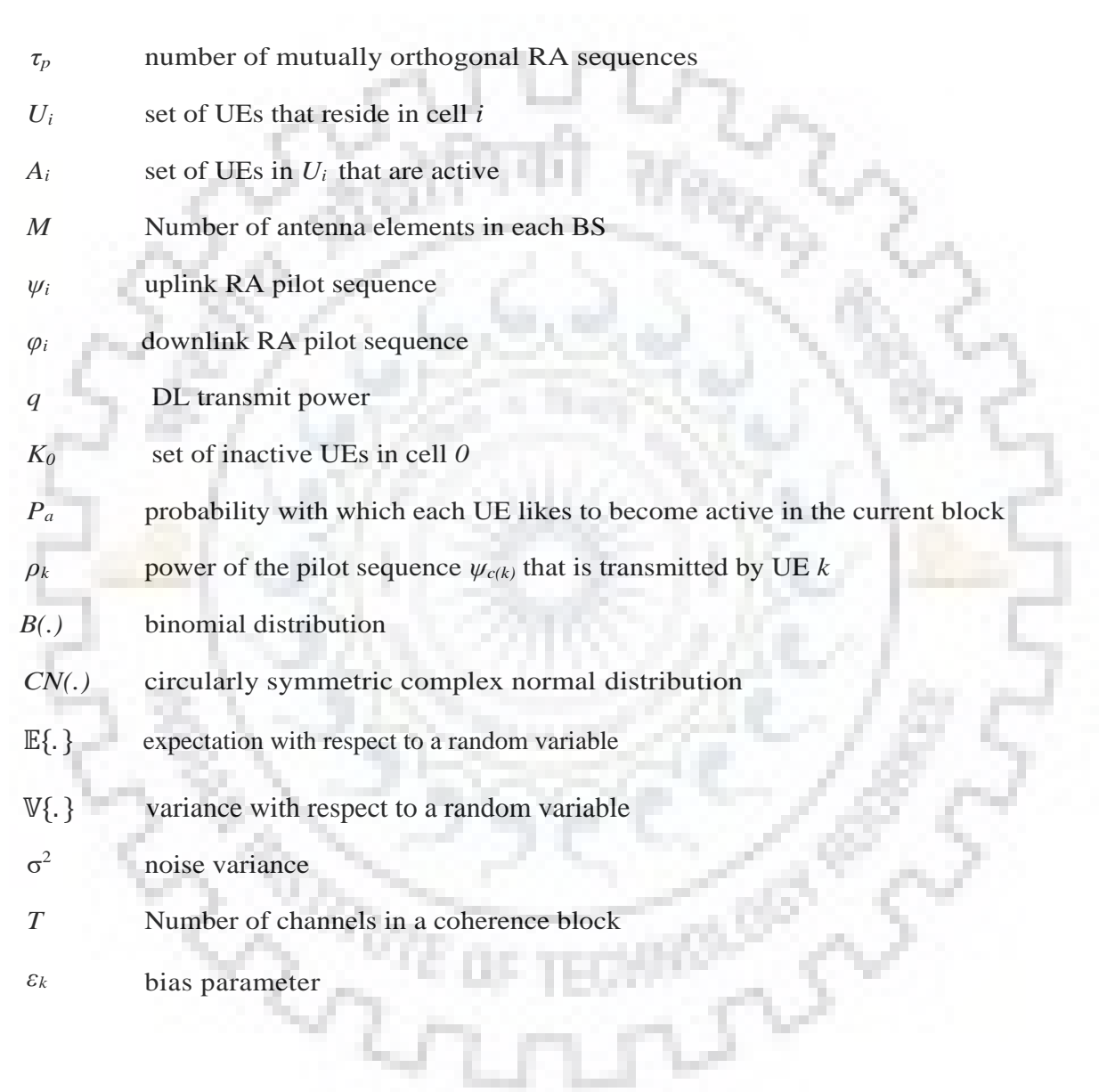


Abbreviations



MIMO	M ultiple I nput M ultiple O utput
UE	U ser E quipments
SUCRe	S trongest U ser C ollision R esolution
SNR	S ignal to N oise R atio
TDD	T ime D ivision M ultiplexing
NMSE	N ormalized M ean S quare E rror
5G	5th G eneration
LTE	L ong T erm E volution
PRACH	P hysical R andom A ccess C hannel
BS	B ase S tation
RRC	R adio R esource C ontrol
RA	R andom A ccess
OFDM	O rthogonal F requency D ivision M ultiplexing
UL	U plink
DL	D ownlink
CP	C yclic P refix
ML	M aximum L ikelihood

Symbols



τ_p	number of mutually orthogonal RA sequences
U_i	set of UEs that reside in cell i
A_i	set of UEs in U_i that are active
M	Number of antenna elements in each BS
ψ_i	uplink RA pilot sequence
ϕ_i	downlink RA pilot sequence
q	DL transmit power
K_0	set of inactive UEs in cell 0
P_a	probability with which each UE likes to become active in the current block
ρ_k	power of the pilot sequence $\psi_{c(k)}$ that is transmitted by UE k
$B(\cdot)$	binomial distribution
$CN(\cdot)$	circularly symmetric complex normal distribution
$\mathbb{E}\{\cdot\}$	expectation with respect to a random variable
$\mathbb{V}\{\cdot\}$	variance with respect to a random variable
σ^2	noise variance
T	Number of channels in a coherence block
ε_k	bias parameter

Chapter 1

Introduction

1.1 Motivation

The massive multiple-input multiple-output (MIMO) systems deliver services for a huge number of user equipments (UEs) simultaneously, by using a massive number of antenna elements at the base station (BS), which makes it potentially viable to manage the explosion of wireless data traffic. Hence it is one of the key technologies for the fifth-generation (5G) time-division-duplex (TDD) communication system. The speed with which we are becoming a fully networked society, the number of wirelessly linked devices and their corresponding data traffic flow are bound to grow by that rate. This growth rate is driven by video streaming, social networking and new technologies like machine-to-machine communication and internet of things. However, the current network infrastructure is unable to avoid all the congestion that will occur in a few years hence will not be able to ensure service quality and availability. Thus the future cellular networks that will be deployed in urban areas need to handle a massive number of connected UEs that will be requesting massive data volumes.

This capacity upgradation is possible only by improving spectral efficiency. The basic fundamental block of traffic which is data packets are often created in a sporadic and irregular manner (for example non-streaming applications which are characterized by bursty on-off traffic). To deal with such irregular switching between UE and BS, the Strongest User Collision Resolution (SUCRe) protocol was developed [35] which was able to resolve up to 90% collisions successfully. However, when the path loss differences between the contending UEs were not noticeably large (which is the requirement of hard decision rule used in step 3 as explained in chapter 3) the performance starts deteriorating. This work focuses on these limitations of SUCRe protocol i.e. when the path loss differences between the UEs using the same pilots is not significantly large, this protocol fails to assign any one UE as the contention winner.

1.2 Massive MIMO systems

Massive MIMO is a multi-user MIMO system with M antennas and K users per BS. The system is characterized by $M \gg K$ which operates in TDD mode by means of linear uplink and downlink processing.

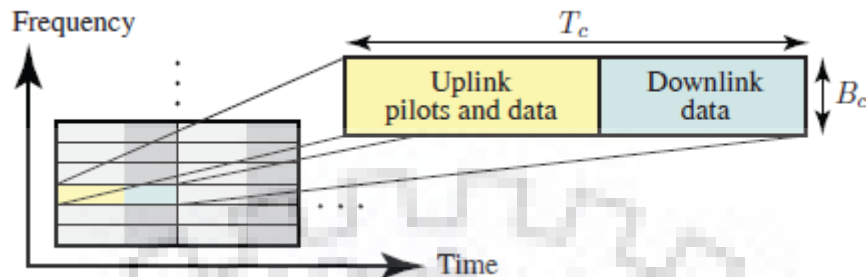


Figure 1: The basic Massive MIMO transmission [41]

Fig. 1 shows the basic Massive MIMO transmission protocol. Here the time-frequency resources are being broken into coherence blocks of size B_c Hz (which is less than or equal to the coherence bandwidth of the channels of the users) and T_c s (which is selected such that it is less than or equal to the coherence time of the channel) such that each user channel becomes approximately frequency flat and static within a block. Each of these coherence intervals is operated in TDD mode and can contain downlink as well as uplink payload transmissions.

1.3 Channel hardening and favorable propagation properties

These two are properties of multi-antenna propagation, which are explained below:

1.3.1 Channel Hardening

One of the key impairments in wireless communication is small scale channel fading, it is actually random fluctuations in the channel gain caused by microscopic changes in the propagation environments. These fluctuations are so unreliable that sometimes, the channel gain is so small that the transmitted data is received in error. Spatial diversity is one of the methods to mitigate the effect of small scale fading. In massive MIMO, the spatial diversity leads to “channel hardening” [36]. Channel hardening makes a fading channel behave as a deterministic channel. In other words, it behaves as if it was a non-fading channel. The randomness due to small-scale fading is still there but its impact will be almost nullified. This property alleviates the need for combating small-scale fading (e.g., by adapting the transmit powers) and improves the DL Channel gain estimation. Channel hardening can be utilized to obtain simpler and more intuitive spectral efficiency (SE) expressions.

Definition (Channel hardening). Asymptotic channel hardening is said to be provided by a propagation channel if

$$\frac{\|h_{jk}^j\|^2}{\mathbf{E}\{\|h_{jk}^j\|^2\}} \rightarrow 1 \quad (1)$$

As number of antennas $M \rightarrow \infty$. This definition says that the gain $\|h_{jk}^j\|^2$ of an arbitrary fading channel h_{jk}^j is close to its mean value when there are many antennas. Channel hardening makes the channel very reliable by making it nearly deterministic which results in lower latency.

1.3.2 Favourable propagation

The propagation is said to be favorable when users are mutually orthogonal in some practical sense. If h and g are two channel vectors corresponding to two users, then they will be orthogonal if $h^H g = 0$. However, it is never possible in real-time systems, but some modifications can be done to define this orthogonality as explained below:

Definition (Favorable propagation). The two channels h and g to BS are said to provide asymptotically favorable propagation if

$$\frac{(h)^H g}{\sqrt{\mathbf{E}\{\|h\|^2 \mathbf{E}\|g\|^2\}}} \rightarrow 0 \quad (2)$$

i.e. the users are practically orthogonal when $\frac{h^H g}{\|h\| \|g\|}$ has zero mean and a variance that is much smaller than one. Favorable propagation makes the directions of two UE channels asymptotically orthogonal. This property makes it easier for the BS to reduce interference between these UEs, which generally improves the SE and makes it sufficient to use linear combining and precoding.

Channel Hardening and Favourable propagation are two related but significantly dissimilar properties. Mostly, a channel can have both of the above properties, one of them or none at all. Massive MIMO does not require or formally rely on any of these properties, but any multiuser MIMO system performs better when the two properties are satisfied.

Chapter 2

Random access protocol in Massive MIMO

Massive MIMO can provide very high spectral efficiency in sub-6 GHz bands. The fundamental thought is to utilize plentiful antennas at BS, which at the same time can serve many devices through spatial multiplexing. In this context, three physical phenomena are important which are described below:

1. Amplification of array gain by spatial capture.
2. Making the channel approximately deterministic by using channel hardening feature.
3. Facilitating spatial multiplexing by maintaining high spatial resolution.

All these three phenomena are used in massive MIMO for random access. The array gain improves the signal-to-noise ratio (SNR), which aids in distinguishing weak devices. Channel hardening property of the channel allows us to exploit asymptotic channel properties. The multiplexing capability suggests the chances of resolving collisions spatially.

2.1 Classification of collision resolution techniques

A device sends a random sequence towards the BS and gets the access whenever it wants. This random sequence which is also called as the pilot sequence is mainly used for estimation of the channel and also to obtain the protected pilot sequence (which is unique in a given cell) for further data transmission in a collision-free environment. A collision is said to occur if two or more users are trying to transmit the same pilot sequence at the same time.

2.1.1 Centralized Collision Resolution Technique

Fig. 2 describes the process involved in centralized collision resolution method. In this technique, the collision discovery at BS is facilitated by coded pilot sequences which consist of non-zero symbols that will be used for estimation of the channel and some null symbols positioned at random positions in the coded pilot sequences which are only used for the collision detection. The method in [38] has been adapted here for collision resolution. Here each device is mapped to a unique on-off pattern. In phase 1, if at BS, the number of silent symbols (off symbols in on-off pattern) is smaller than the null symbols then, a collision has occurred this event will be broadcasted in phase 2 and a new pilot access is

performed in phase 3 (the probability of new collision event is reduced) and access will be granted to the non-colliding devices in phase 4. However, in phase 1, if number of silent symbols and null symbols are equal then no collision will occur and access will be granted immediately.

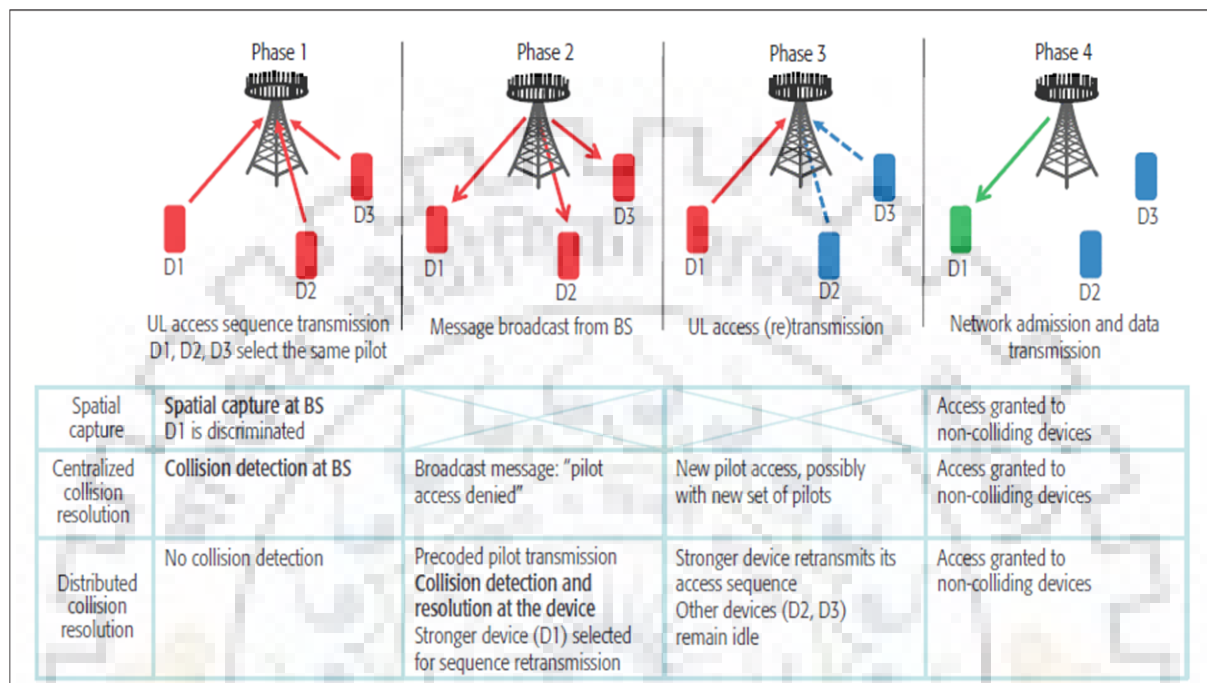


Figure 2: Random access to pilots (RAP) [37]

2.1.2 Distributed Collision Resolution Technique

In this technique, the collision is detected at UE. The BS uses the received signal from phase 1 (Fig. 2) to determine the sum of channel gains of all the contending UEs. BS then use this information to multicast a precoding sequence towards all the contending devices in phase 2. The estimated gains can then be used for distributed collision resolution, by setting a criterion (for example the criterion used in SUCRe protocol [24]) on when a device should retransmit its pilot in phase 3. And then the access will be granted to all the non-colliding users. The main difference between the above two collision resolution technique is that in centralized collision resolution, the collision is detected at BS whereas, in distributed collision resolution method, this collision detection happens at the UE end (Fig. 2).

2.2 Random Access Functionality in LTE

The SUCRe protocol is very similar to the protocol used in the physical random access channel (PRACH) of LTE. Therefore, the PRACH protocol is discussed for the better understanding of the SUCRe protocol. It comprises of four steps (Fig. 3):

- Each accessing UE will randomly select a preamble from the predefined database. As this selection of preambles by the UEs that wish to access the network is a totally uncoordinated task, there might be a collision when more than one UE will choose the same preamble at the same time. However, there is no collision detection in the first step and BS only checks if a particular pilot sequence is active or not.

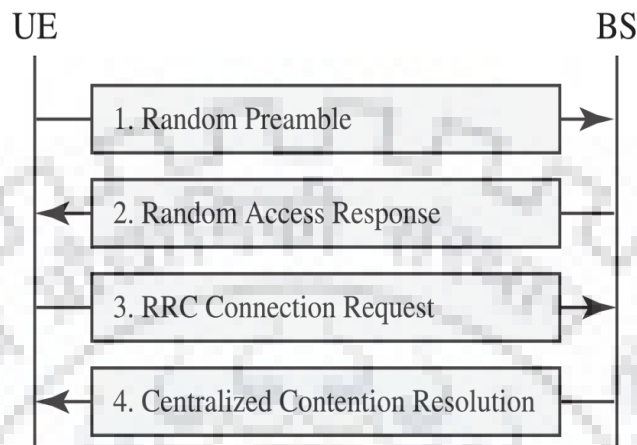


Figure 3: PRACH protocol used in LTE [35]

- The second step comprises of the *random access response* that the BS has sent to every UE that has activated any pilot sequence and allocates resources to them.
- In the third step, an *RRC (Radio Resource Control) connection request* is sent by each UE that has got a random access response (by the BS in step 2) so that subsequent data transmission can happen in further steps. If in the first step, one or more UE have activated the same preamble then those UEs will use the same resources to send the RRC request in the third step also. Thus the event of a collision is registered.
- *Collision resolution* happens in the fourth step which is centralized in manner. This step may contain two or more complex steps to resolve collision.

2.3 Random access functionality in massive MIMO

In conventional cellular networks like LTE, as the traffic is not that great, therefore it was possible to allocate a dedicated resource to every UE that is active. In that case, BS needed to convey the time-frequency positions of these permanently allocated resources but in massive MIMO, instead of sending time-frequency positions of the resources, BS chooses to assign time-frequency resources to all active UEs and separates them spatially with the help of their preambles. According to the basic massive MIMO phenomena explained in [4], the users use mutually orthogonal pilot sequences within the same

cell so that no interference is caused by the UEs residing in the same cell (intra-cell pilot contamination). However, frequency reuse is mandatory which often leads to the inter-cell pilot contamination causing additional interference [8].

In the crowded scenarios, the overall number of UEs (including active as well as inactive UEs) residing in a single cell is much greater than the available number of preambles (and it is not possible to have as many numbers of pilot sequences as the number of UEs). Also, the data traffic flow is of irregular and intermittent fashion so it will be illogical to allocate a pilot to a UE permanently when it will be sending its data only for a short duration, and for the rest of the time, it will be sitting idle. These pilot sequences have to be allocated opportunistically rather than permanently. This can be done by employing some random access mechanism. However, the collision might take place in crowded case if pilots are accessed randomly by the UEs which leads to intra-cell pilot contamination at the cost of reduced access delays as explained [19]- [21]. Therefore, a suitable collision detection and resolution technique should also be incorporated in the random access mechanism. This is achieved by using “*SUCRe (strongest user collision resolution) protocol*” [35]. This is a scalable protocol and works on the distributed Collision resolution technique. It has been able to resolve intra-cell pilot collisions up to 90% successfully.



Chapter 3

Conventional SUCR (Strongest User Collision Resolution) protocol

3.1 General considerations

A cellular network is considered where each BS has M antennas. The time-frequency resources are broken into blocks with coherence time of T (Fig.1) such that channel response between the BS and UE remains constant and frequency flat within that block U_i is the set of all the UEs residing in cell i , out of which only A_i UEs are active at any given instant. Here the crowded urban case is taken (very large number of UE: $|U_i| \gg T$) but the active UEs satisfy $|A_i| < T$, thus the BS can provisionally allot orthogonal preambles to these UEs.

The coherence blocks have been further broken into two classes according to their functionality as shown in Fig. 4:

- *Payload data blocks*: The payload data blocks are used for uplink and downlink data transmission to the UEs in the set A_i for each cell i . For the time being, these UEs have been assigned $|A_i|$ mutually orthogonal pilots. These pilots will also be reused in other cells (the frequency reuse factor is chosen such that the pilot contamination is minimized [5])
- *Random access blocks*: The random access blocks will only be used by the UEs which are inactive, for the random access (i.e., those which are in the set in U_i/A_i) that desire to be admitted to the payload data blocks; that is, to be assigned a momentarily pilot which will be dedicated to a particular UE for a short duration. SUCRe protocol works on these RA blocks.

In Fig. 4, it can be seen that the random access blocks are positioned differently between the adjacent cells (by implementing the reuse factor of 3). These RA blocks can either remain inactive or be inactive and send payload data during the random access. This kind of categorization has been done to avoid inter-cell interference.

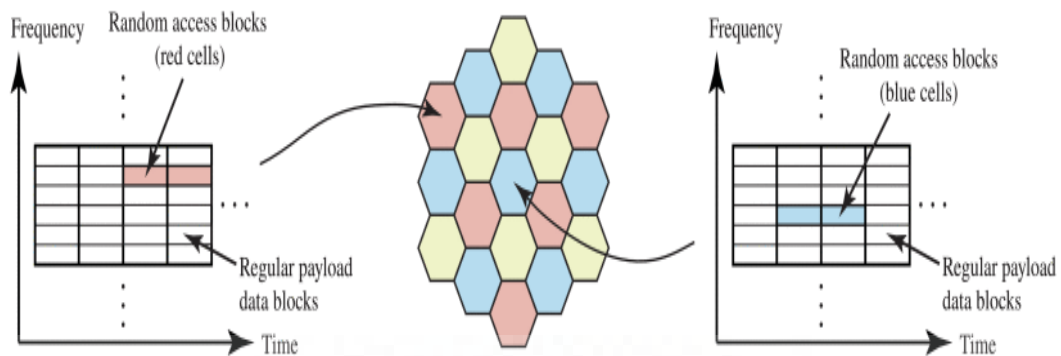


Figure 4: Division of time-frequency domain into coherence intervals in SUCRe protocol [35]

3.2 SUCR overview

The steps involved in the conventional SUCRe are described below:

- *Step 0:* BS broadcasts a control signal which is used by the UEs to estimate their respective channel gains and synchronize themselves with the BS for further communication.
- *Step 1:* Any UE that wants to send data picks a pilot sequence from a predefined set of random access sequences in a random fashion. BS i use this pilot to estimate the channel used by that particular UE to send that pilot sequence. If more than one UE have chosen the same random access pilot accidentally from the pool, the BS will estimate the superposition of all those channels over which these pilots have been propagated over by those UEs. However, there will be no detection of collision in the first step.

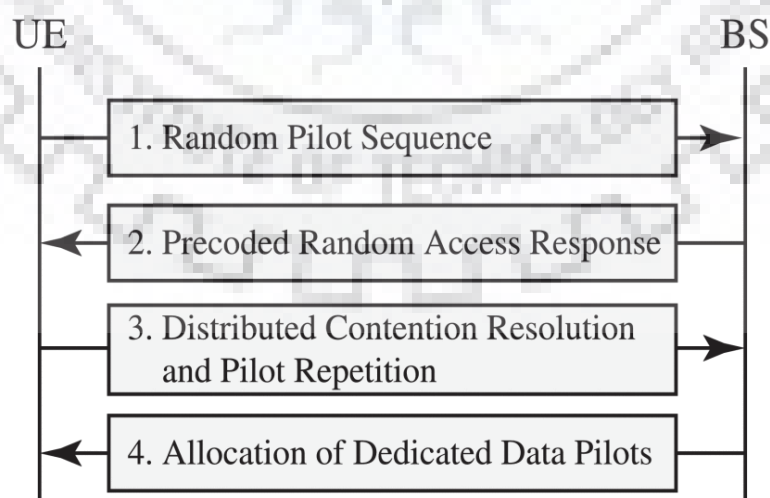


Figure 5: conventional SUCRe protocol

- *Step 2:* Using the channel estimates calculated in step 1, BS forms a precoding vector and sends the downlink (DL) pilots using these vectors. Because of such precoding, the signal will be spatially directed towards the respective UEs which have sent those particular pilots.
- *Step 3:* Retransmission of the RA pilot sequence along with the UE identity information of a request for further data transmission is done in the third step by employing a rule that “only the UE that has strongest signal gain will appoint itself as a contention winner, and should repeat the pilot.” Thus detection, as well as resolution of any collision, will be done in the third step.
- *Step 4:* The resources that have been requested in the third step by the UEs are granted in step 4 by allocating them a protected pilot sequence that is unique.

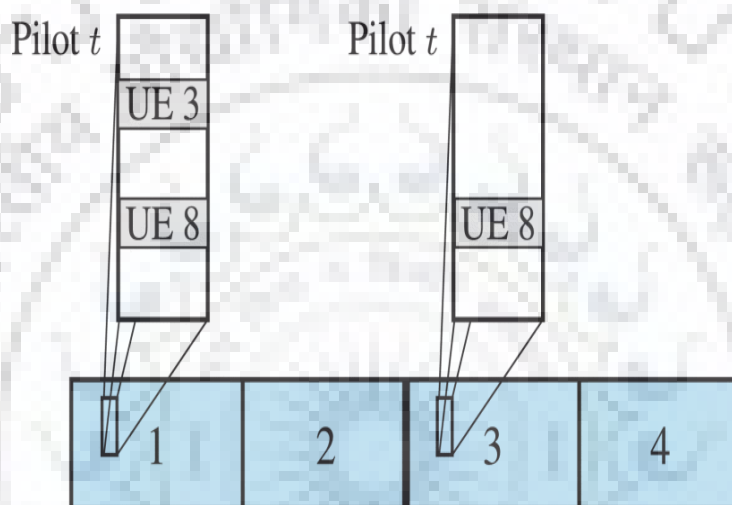


Figure 6: Retransmission of the strongest UE is done in the third step [35]

Table 1: Difference between PRACH and SUCRe protocol

PRACH	SUCRe
<ul style="list-style-type: none"> • In LTE, all UEs that have sent the same RA pilot in the first step will retransmit their pilot in the third step also. 	<ul style="list-style-type: none"> • In SUCRe, the retransmission of RA pilot in the third step will be done by only that UE which has the strongest signal gain among all the contenders.
<ul style="list-style-type: none"> • More pilots will be colliding, so overall throughput is lower than SUCRe. 	<ul style="list-style-type: none"> • Thus there is a significant increment in the probability of non-colliding pilot transmission as compared to the PRACH protocol.
<ul style="list-style-type: none"> • Collision is detected at BS in a centralized way. 	<ul style="list-style-type: none"> • Collision is detected at UE end in a distributed way.

3.3 System Model of the SUCRe protocol

Consider an arbitrary cell that has a predefined number of inactive UEs. Let K_0 denote the number of inactive UEs in cell 0 . These K_0 user equipment are supposed to share τ_p mutually orthogonal random access pilots $\boldsymbol{\psi}_1, \dots, \boldsymbol{\psi}_{\tau_p} \in \mathbb{C}^{\tau_p}$ that span τ_p UL channel uses and satisfy $\|\boldsymbol{\psi}_t\|^2 = \tau_p$.

Each of the K_0 UEs selects one of the τ_p pilot sequences homogenously in each RA block in a random fashion: UE k selects pilot $c(k) \in \{1, 2, \dots, \tau_p\}$. $P_a \leq 1$ is the probability with which each UE would like to become active. UE k tries to access the network by sending the pilot $\boldsymbol{\psi}_{c(k)}$ with power $\rho_k > 0$, otherwise, it will remain quiet by setting $\rho_k = 0$. The set $\mathcal{S}_t = \{k: c(k) = t, \rho_k > 0\}$ comprises of all the UEs that have transmitted pilot t . P_a/τ_p denotes the probability with which a UE wishes to send data by sending a particular pilot $\boldsymbol{\psi}_t$. These inactive UEs, $|\mathcal{S}_t|$ that will be transmitting $\boldsymbol{\psi}_t$ have a binomial distribution [35]:

$$|\mathcal{S}_t| \sim B(K_0, \frac{P_a}{\tau_p}). \quad (3)$$

By expanding the binomial expression in (3), we can obtain the probability of collision ($|\mathcal{S}_t| \geq 2$) that happens between the UEs that have chosen the pilot $\boldsymbol{\psi}_t$ as follows [35]:

$$1 - (1 - \frac{P_a}{\tau_p})^{K_0} - K_0 \frac{P_a}{\tau_p} (1 - \frac{P_a}{\tau_p})^{K_0-1}. \quad (4)$$

where the second term represents the probability when the pilot $\boldsymbol{\psi}_t$ is unused ($|\mathcal{S}_t| = 0$), and the third term denotes the probability when $\boldsymbol{\psi}_t$ is selected by only one UE ($|\mathcal{S}_t| = 1$).

Thus The channel vector between UE $k \in \mathcal{K}_0$ and its BS is indicated by $\mathbf{h}_k \in \mathbb{C}^M$. A general propagation model has been adapted, where the channels are assumed to satisfy *channel hardening* and *asymptotic favorable propagation* [25] properties depicted in (5) and (6) respectively [35].

$$\frac{\|\mathbf{h}_k\|^2}{M} \xrightarrow{M \rightarrow \infty} \beta_k, \forall k, \quad (5)$$

$$\frac{\mathbf{h}_k^H \mathbf{h}_i}{M} \xrightarrow{M \rightarrow \infty} 0, \forall k, i, k \neq i, \quad (6)$$

The mathematical modeling of the four steps of SUCRe protocol is done below:

1) Random Pilot Sequence:

Firstly, when any UE wants to become active, it sends a random pilot sequence towards the BS. The BS obtains the signal $\mathbf{Y} \in \mathbb{C}^{M \times \tau_p}$ from the pilot transmission of UEs [35]:

$$\mathbf{Y} = \sum_{k \in \mathcal{K}_0} \sqrt{\rho_k} \mathbf{h}_k \boldsymbol{\psi}_{c(k)}^T + \mathbf{W} + \mathbf{N}, \quad (7)$$

where the matrix $\mathbf{N} \in \mathbb{C}^{M \times \tau_p}$ represents independent receiver noise coefficients where each element is distributed as circularly symmetric complex Gaussian distribution ($\mathcal{CN}(0, \sigma^2)$), $\mathbf{W} \in \mathbb{C}^{M \times \tau_p}$ represents interference from other cells.

The BS obtains \mathbf{y}_t by correlating \mathbf{Y} with an arbitrary (normalized) pilot sequence $\boldsymbol{\psi}_t$ [35]

$$\begin{aligned} \mathbf{y}_t &= \mathbf{Y} \frac{\boldsymbol{\psi}_t^*}{\|\boldsymbol{\psi}_t\|} = \sum_{i \in \mathcal{S}_t} \sqrt{\rho_i} \|\boldsymbol{\psi}_t\| \mathbf{h}_i + \mathbf{W} \frac{\boldsymbol{\psi}_t^*}{\|\boldsymbol{\psi}_t\|} + \mathbf{n}_t \\ \mathbf{y}_t &= \sum_{i \in \mathcal{S}_t} \sqrt{\rho_i \tau_p} \mathbf{h}_i + \mathbf{W} \frac{\boldsymbol{\psi}_t^*}{\|\boldsymbol{\psi}_t\|} + \mathbf{n}_t, \end{aligned} \quad (8)$$

where $\mathbf{n}_t = \mathbf{N} \frac{\boldsymbol{\psi}_t^*}{\|\boldsymbol{\psi}_t\|} \sim \mathcal{CN}(\mathbf{0}, \sigma^2 \mathbf{I}_M)$ is the effective receiver noise. Now, \mathbf{W} which depicts the interference part is mathematically described as [35],

$$\mathbf{W} = \sum_l \mathbf{w}_l \mathbf{d}_l^T + \sum_{t=1}^{\tau_p} \sum_{k \in \mathcal{S}_t^{\text{interf}}} \sqrt{\rho_{t,k}} \mathbf{g}_{t,k} \boldsymbol{\psi}_t^T. \quad (9)$$

The above equation comprises of two parts. The first summation denotes the interference from the data transmissions from neighbor cells that use a different resource block in cell 0 (in time-frequency domain). The l^{th} interferer which is using the channel $\mathbf{w}_l \in \mathbb{C}^M$ transmits some random data sequence $\mathbf{d}_l \in \mathbb{C}^{\tau_p}$. The second summation refers to the interferers in neighboring cells using the same resource block as the RA block in cell 0 , which perform random access. These interferers that use pilot $\boldsymbol{\psi}_t$ are clubbed in the set $\mathcal{S}_t^{\text{interf}}$, and member $k \in \mathcal{S}_t^{\text{interf}}$ having the $\mathbf{g}_{t,k}$ will be using the transmit power $\rho_{t,k}$. [35]

$$\mathbf{w} \frac{\boldsymbol{\psi}_t^*}{\|\boldsymbol{\psi}_t\|} = \sum_l \mathbf{w}_l \frac{\mathbf{d}_l^T \boldsymbol{\psi}_t^*}{\|\boldsymbol{\psi}_t\|} + \sum_{k \in \mathcal{S}_t^{\text{interf}}} \sqrt{\rho_{t,k} \tau_p} \mathbf{g}_{t,k}. \quad (10)$$

$$\left| \mathbf{w} \frac{\boldsymbol{\psi}_t^*}{\|\boldsymbol{\psi}_t\|} \right|^2 = \sum_l \mathbf{w}_l \frac{|\mathbf{d}_l^T \boldsymbol{\psi}_t^*|^2}{\|\boldsymbol{\psi}_t\|^2} + \sum_{k \in \mathcal{S}_t^{\text{interf}}} (\sqrt{\rho_{t,k} \tau_p} \mathbf{g}_{t,k})^2 + 2 \sum_l \mathbf{w}_l \frac{\mathbf{d}_l^T \boldsymbol{\psi}_t^*}{\|\boldsymbol{\psi}_t\|} \sum_{k \in \mathcal{S}_t^{\text{interf}}} \sqrt{\rho_{t,k} \tau_p} \mathbf{g}_{t,k}. \quad (11)$$

If the interfering channels are also assumed to satisfy channel hardening and Favourable propagation properties described in (5) and (6), for $M \rightarrow \infty$, denoted as $\|\mathbf{w}_l\|^2/M \rightarrow \beta_{w,l}$ and $\|\mathbf{g}_{t,k}\|^2/M \rightarrow \beta_{t,k}$, (11) can be written as ,

$$\omega_t = \frac{\left| \mathbf{w} \frac{\boldsymbol{\psi}_t^*}{\|\boldsymbol{\psi}_t\|} \right|^2}{M} \rightarrow \sum_l \beta_{w,l} \frac{|\mathbf{d}_l^T \boldsymbol{\psi}_t^*|^2}{\|\boldsymbol{\psi}_t\|^2} + \sum_{k \in \mathcal{S}_t^{\text{interf}}} \rho_{t,k} \tau_p \beta_{t,k} \quad (12)$$

The third term in (11) vanishes as $M \rightarrow \infty$ according to (6). Although ω_t contains interference caused by data transmission as well as RA pilots in other cells, but the interference caused by the data transmission will play the dominant role because of the neighboring cells which are the closest in time-frequency domain send data.

2) Precoded Random Access Response from BS towards the UE:

The second step involves the response from BS to the RA pilots sent by UE. This response is a precoded downlink pilot signal corresponding to each RA pilot that was sent in the first step by the UE. $\boldsymbol{\phi}_t \in \mathbb{C}^{\tau_p}$ is the downlink pilot corresponding to $\boldsymbol{\psi}_t$. These downlink pilots $\boldsymbol{\phi}_1, \dots, \boldsymbol{\phi}_{\tau_p} \in \mathbb{C}^{\tau_p}$ are mutually orthogonal and satisfy $\|\boldsymbol{\phi}_t\|^2 = \tau_p$. The precoded downlink pilot signal $\mathbf{V} \in \mathbb{C}^{M \times \tau_p}$ is [35]

$$\mathbf{V} = \sqrt{q} \sum_{t=1}^{\tau_p} \frac{\mathbf{y}_t^*}{\|\mathbf{y}_t\|} \boldsymbol{\phi}_t^T, \quad (13)$$

similar to the uplink transmit power ρ , q is the downlink transmit power whose value is predefined.

The signal $\mathbf{z}_k \in \mathbb{C}^{\tau_p}$ received by the some UE $k \in \mathcal{S}_t$ is [35]

$$\mathbf{z}_k^T = \mathbf{h}_k^T \mathbf{V} + \mathbf{v}_k^T + \boldsymbol{\eta}_k^T, \quad (14)$$

where \mathbf{h}_k^T is the reciprocal downlink channel, \mathbf{v}_k represents unter-cell interference and $\boldsymbol{\eta}_k \sim \mathcal{CN}(\mathbf{0}, \sigma^2 \mathbf{I}_{\tau_p})$ is the receiver noise. By correlating the received signal \mathbf{z}_k with the normalized

DL pilot sequence $\boldsymbol{\phi}_t$, (14) can be modified as,

$$z_k = \mathbf{z}_k^T \frac{\boldsymbol{\phi}_t^*}{\|\boldsymbol{\phi}_t\|} = \mathbf{h}_k^T \mathbf{V} \frac{\boldsymbol{\phi}_t^*}{\|\boldsymbol{\phi}_t\|} + \mathbf{v}_k^T \frac{\boldsymbol{\phi}_t^*}{\|\boldsymbol{\phi}_t\|} + \boldsymbol{\eta}_k^T \frac{\boldsymbol{\phi}_t^*}{\|\boldsymbol{\phi}_t\|} \quad (15a)$$

Substituting the value of \mathbf{V} from (13), (15-a) can be written as,

$$z_k = \mathbf{z}_k^T \frac{\boldsymbol{\phi}_t^*}{\|\boldsymbol{\phi}_t\|} = \sqrt{q} \mathbf{h}_k^T \frac{\boldsymbol{\phi}_t^*}{\|\boldsymbol{\phi}_t\|} \boldsymbol{\phi}_t^T \frac{\mathbf{y}_t^*}{\|\mathbf{y}_t\|} + \mathbf{v}_k^T \frac{\boldsymbol{\phi}_t^*}{\|\boldsymbol{\phi}_t\|} + \boldsymbol{\eta}_k^T \frac{\boldsymbol{\phi}_t^*}{\|\boldsymbol{\phi}_t\|} \quad (15b)$$

Again putting $\boldsymbol{\phi}_t^* \boldsymbol{\phi}_t^T = \|\boldsymbol{\phi}_t\|^2 = \tau_p$, the above equation becomes

$$z_k = \mathbf{z}_k^T \frac{\boldsymbol{\phi}_t^*}{\|\boldsymbol{\phi}_t\|} = \sqrt{q\tau_p} \mathbf{h}_k^T \frac{\mathbf{y}_t^*}{\|\mathbf{y}_t\|} + \mathbf{v}_k^T \frac{\boldsymbol{\phi}_t^*}{\|\boldsymbol{\phi}_t\|} + \eta_k \quad (15c)$$

where $\eta_k = \boldsymbol{\eta}_k^T \frac{\boldsymbol{\phi}_t^*}{\|\boldsymbol{\phi}_t\|} \sim \mathcal{CN}(0, \sigma^2)$ is the effective receiver noise. Also,

$$\begin{aligned} \frac{z_k}{\sqrt{M}} &= \frac{\sqrt{q\tau_p} (\mathbf{h}_k^H \mathbf{y}_t)^*}{M} \frac{1}{\sqrt{\frac{1}{M} \|\mathbf{y}_t\|^2}} + \frac{\mathbf{v}_k^T \boldsymbol{\phi}_t^*}{\sqrt{M} \|\boldsymbol{\phi}_t\|} + \frac{\eta_k}{\sqrt{M}} \\ \frac{z_k}{\sqrt{M}} &\xrightarrow{M \rightarrow \infty} \frac{\sqrt{\rho_k q \beta_k \tau_p}}{\sqrt{\sum_{i \in \mathcal{S}_t} \rho_i \beta_i \tau_p + \omega_t + \sigma^2}} \end{aligned} \quad (16)$$

Noise remains constant with M and the inter-cell interference part \mathbf{v}_k is assumed to be remain unaffected by M because of the previously made assumption that closest interfering cells that will be transmitting the RA pilot will allocate the downlink pilots in a different fashion in order to avoid the interference caused by contamination by coherent pilots. Let us define a new variable α_t as

$$\alpha_t = \sum_{i \in \mathcal{S}_t} \rho_i \beta_i \tau_p + \omega_t \quad (17)$$

Let $\Re(\cdot)$ denote the real part of its input quantity. Substituting this value of α_t in (16), the following estimate can be drawn [35],

$$\frac{\Re(z_k)}{\sqrt{M}} \approx \frac{\sqrt{\rho_k q \beta_k \tau_p}}{\sqrt{\alpha_t + \sigma^2}}, \quad (18)$$

As the imaginary part of z_k comprises only of noise, interference and estimation errors .So they have been discarded conveniently. Based on (17), UE k estimates α_t as follows [35]:

$$\hat{\alpha}_{t,k}^{\text{approx1}} = \max\left(\frac{M q \rho_k \beta_k^2 \tau_p^2}{(\Re(z_k))^2} - \sigma^2, \rho_k \beta_k \tau_p\right), \quad (19)$$

Here $\max(\cdot, \cdot)$ selects the maximum of the two values (since UE k knows that $\alpha_t \geq \rho_k \beta_k \tau_p$).

3) Collision Resolution and Pilot Retransmission by the UE

Pilot retransmission is done in the third step. Each UE $k \in \mathcal{S}_t$ is well aware of its own average signal gain $\rho_k \beta_k \tau_p$ and the sum of signal gains of the other contenders (plus inter-cell interference) that leads to the deduction of following *hard decision rule*:

- Pilot collision is said to occur when $\hat{\alpha}_{t,k} > \rho_k \beta_k \tau_p$
- It can also determine the amount by which it's signal gain is stronger than the cumulative sum of its contenders: $\rho_k \beta_k \tau_p / \hat{\alpha}_{t,k}$

The contentions are resolved considering the following rules:

Rule 1:

The UE $k \in \mathcal{S}_t$ with the largest $\rho_k \beta_k \tau_p$, will be regarded as the winner of contention, also called as the *strongest user*.

Considering the instant when α_t is known exactly (i.e. asymptotic case), if k^{th} UE's signal gain is greater than the sum of signal gains of all other contending UEs, then it will definitely be the winner of contention. This can be modelled mathematically as [35]

$$\begin{aligned} \rho_k \beta_k \tau_p &> \alpha_t - \rho_k \beta_k \tau_p \\ \rho_k \beta_k \tau_p &> \alpha_t / 2 \end{aligned} \quad (20)$$

Rule 2:

A collision is said to be resolved if and only if one UE regards itself as the contention winner.

Rule 3:

When any single UE is unable to appoint itself a contention winner then a *false negative* occurs whereas more than one UE tries to appoint itself as the strongest UE, a *false positive* occurs.

The following distributed *hard decision rule* is used by the UEs [35]:

$$\mathcal{R}_k: \rho_k \beta_k \tau_p > \hat{\alpha}_{t,k} / 2 + \epsilon_k (\text{repeat}), \quad (21)$$

$$\mathcal{J}_k: \rho_k \beta_k \tau_p \leq \hat{\alpha}_{t,k} / 2 + \epsilon_k (\text{inactive}). \quad (22)$$

If \mathcal{R}_k is true, UE $k \in \mathcal{S}_t$ concludes that it has the strongest signal gain and *retransmits* the pilot ψ_t in Step 3. However, if \mathcal{J}_k is true, it remains silent. False positives and false negatives are caused mostly by the errors in estimation and inter-cell interference. The final performance of the system can be altered by some adjustments in the bias parameter $\epsilon_k \in \mathbb{R}$.

The probability of resolving a collision can be evaluated using (21) and (22) as done in [35]:

$$P_{|\mathcal{S}_t| \text{ resolved}} = \Pr\{\mathcal{R}_1, \mathcal{J}_2, \dots, \mathcal{J}_{|\mathcal{S}_t|}\} + \Pr\{\mathcal{J}_1, \mathcal{R}_2, \mathcal{J}_3, \dots, \mathcal{J}_{|\mathcal{S}_t|}\} + \dots \quad (23)$$

$$+ \Pr\{\mathcal{J}_1, \dots, \mathcal{J}_{|\mathcal{S}_t|-1}, \mathcal{R}_{|\mathcal{S}_t|}\},$$

4) Temporary Allocation of Dedicated and Unique Pilots Sequences to the UEs by BS:

The retransmitted RA pilot along with some other uplink messages are received by the BS in the third step. BS uses ϕ_t for estimating the channel of the UE that has transmitted RA pilot ψ_t and the message associated with that RA pilot is decoded . Once this process of decoding is completed successfully (it denotes that BS has recognized one of the inactive UEs that have transmitted the same RA pilot ψ_t in step 1), BS can add it to the payload data blocks by assigning pilot sequence ψ_t to that UE for further data transmission. This resource allocation decision is transmitted to UE in the downlink signal.

The above four steps in the SUCRe protocol are repeated at a given interval. The UEs that are not allocated a unique pilot sequence in step 4 will be trying for the random access again after some time. However, the fashion in which they will be again repeating this process can be decided. Alternatively, additional steps on top of the SUCRe protocol also can be added to resolve the remaining collisions (like SUCR-TA (strongest user collision resolution with timing advance information) or SUCR-IPA (SUCR combined idle pilot access), by utilizing any conventional contention resolution method.

Chapter 4

Retransmission Based on “Soft Decision Rule”

The SUCRe has been able to resolve a significant portion of the pilot collision in crowded massive MIMO scenarios and continues to admit the UEs efficiently in overloaded networks (shown in chapter 5) but it also has a limitation. As it is based on the “*the strongest user will be the winning contender*” phenomena- *hard decision rule*, there has to be a noticeable difference between the large scale fading coefficient, so this decision rule holds true for only one contending UE. When the number of contenders is not so large, this condition is generally gets satisfied by a few cases whenever a collision occurs. On the contrary, the occurrence of collision is more frequent when the number of UEs within the cell increases, hence the probability that strongest user’s signal gain is higher than half of the sum of other contending UEs signal gain decreases, resulting in no retransmission of pilot signal in step 3 by any UE.

This limitation gives the scope for a different decision rule that can be used for retransmission of pilots in the third step. Conventionally, the SUCRe protocol uses a hard decision rule for this purpose, i.e. if the condition is true, the strongest UE will retransmit its pilot and if not, the UE remains silent which has been described in chapter 3.

4.1 Proposed “Soft Decision Rule”

The k th user will retransmit its chosen pilot in step 3 if the *hard decision rule* in (21) is satisfied.

$$\rho_k \beta_k \tau_p > \hat{\alpha}_{t,k}/2 + \epsilon_k \quad (24)$$

Hereby defining $\gamma_{t,k} = \hat{\alpha}_{t,k} + 2\epsilon_k$, equation (20) can be rewritten as ,

$$\frac{\rho_k \beta_k \tau_p}{\gamma_{t,k}} > 0.5, \text{ if } \gamma_{t,k} \text{ is positive} \quad (25)$$

and

$$\frac{\rho_k \beta_k \tau_p}{-\gamma_{t,k}} > -0.5, \text{ if } \gamma_{t,k} \text{ is negative} \quad (26)$$

combining the expressions in (25) and (26),

$$\frac{\rho_k \beta_k \tau_p}{|\gamma_{t,k}|} > \text{sign}(\gamma_{t,k})0.5, \quad (27)$$

where $\text{sign}(\cdot)$ is the signum operator.

When the SUCRe decentralized hard decision rule rewritten in (27) holds true then the UE retransmits its sequence. However, this criterion may lead to contradictory conclusions as explained below:

- If the value of $\frac{\rho_k \beta_k \tau_p}{|\gamma_{t,k}|}$ for a given UE approaches $\text{sign}(\gamma_{t,k})0.5$ by the left side, the UE will decide to remain inactive in step 3.
- If it approaches $\text{sign}(\gamma_{t,k})0.5$ from right side, UE will retransmit its pilot in step 3.

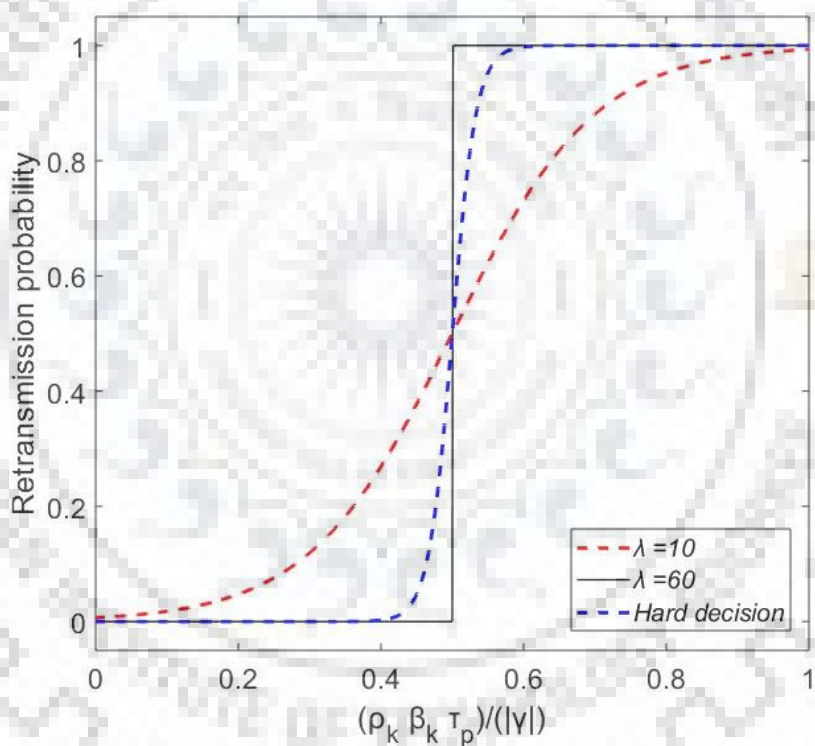


Figure 7: Probability of retransmission based on the conventional hard decision and proposed “soft decision rule”

Moreover, when more UEs that end up contending for the same pilot, their large scale coefficients don't differ by a significant value, so it becomes very difficult for the UEs to appoint themselves as contention winner based on the hard decision rule, this condition leads to false negatives.

Here a soft decision rule is proposed for the SUCRe protocol where the value of $\frac{\rho_k \beta_k \tau_p}{|\gamma_{t,k}|}$ can be mapped into a probability of retransmission for each UE such that its decentralized and uncoordinated

features remain intact. *Sigmoid function* is used for smoothening of the hard decision in (21) as shown in Fig. 8.

A sigmoid function refers to the special case of the logistic function and defined by

$$f(x) = \frac{1}{1 + e^{-\lambda x}}, \forall x \in \mathfrak{R}. \quad (28)$$

Where λ is the smoothening parameter of the sigmoid curve. As the value of λ increases, the curve becomes sharper. This parameter should be chosen carefully so that a suitable performance for any K_0 value can be achieved efficiently.

Here only the positive values of $\gamma_{t,k}$ is taken. When $\gamma_{t,k}$ value is negative, this soft decision curve in Fig. 7 will be shifted horizontally and will be centered at -0.5.



Chapter 5

Performance evaluation and numerical results

The conventional SUCRe protocol is numerically studied in this chapter. Its performance over cellular networks in different fading scenarios are then compared. The performance improvement of SUCRe protocol by using the proposed *soft decision rule* is studied as well. The results of those comparisons will lay the base of these protocols in real-world crowded cellular networks.

A. Performance Comparison of the Conventional SUCRe Protocol Over Different Fading Channels

5.1 Simulation setup

The center cell of the network shown in Fig. 4 is chosen for simulation here. The radius of each cell is 250m and the distance between any two UEs is greater than 25m. they are distributed uniformly with respect to the BS. The estimate $\hat{\alpha}_{t,k}^{\text{approx1}}$ of α_t which is defined in (18) is used in all the simulations.

5.1.1 Channel Propagation Models

A model is necessary to predict the effects of the fading accurately in order to mitigate its effects. Therefore, eight different channel models are taken here. The properties of these channels are as follows:

1) Rayleigh fading channel model

The fading can be modeled as Rayleigh distributed when there is no line of sight (LOS) component present in the received signal. LOS signal may also be characterized by a component that contains considerably higher power than the collective power of all the remaining components.

The probability density function (PDF) of the fading amplitude can be given by (29)

$$p_X(x) = \frac{2x}{\Omega} e^{-\frac{x^2}{\Omega}}, x \geq 0 \quad (29)$$

Where $\Omega = E(X^2)$ is known as fading power.

However, the uncorrelated and correlated fading, both are considered separately while doing the simulations.

2) Hoyt fading channel model

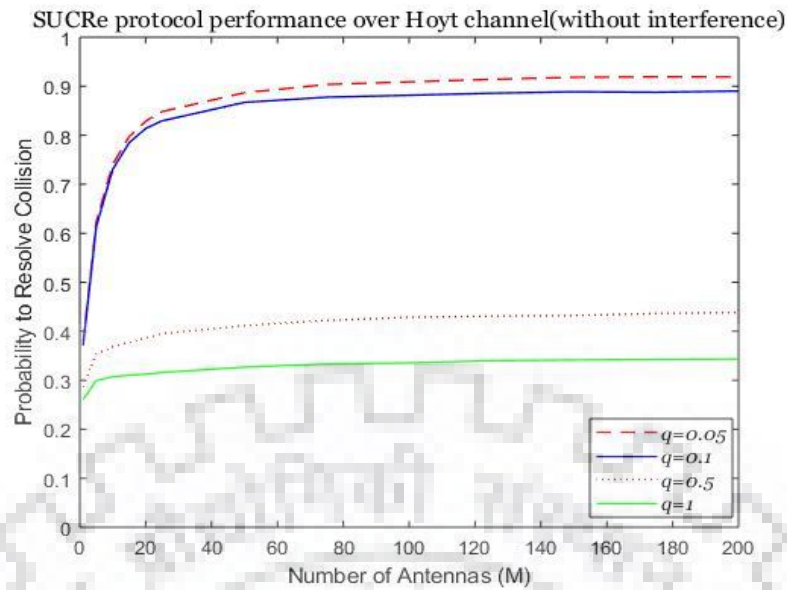
Hoyt distribution is used to model the fading channels when it is more severe than the Rayleigh fading conditions. It is also known as Nakagami- q fading.

$$p_X(x) = \frac{1+q^2}{\Omega} x e^{-\frac{(1+q^2)x^2}{4q^2\Omega}} I_0\left(\frac{1-q^4}{4q^2\Omega} x^2\right), x \geq 0, \quad (30)$$

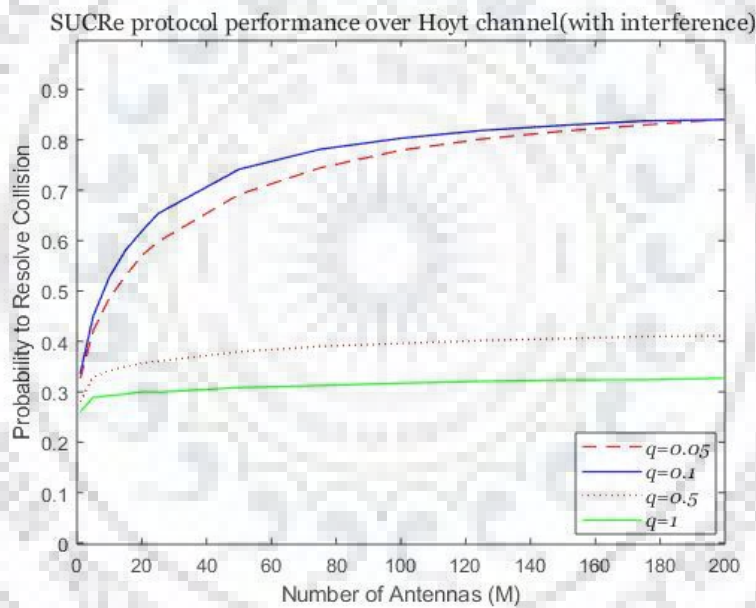
Where q is the fading parameter for Hoyt distribution and I_v is the Bessel function of the first kind and v^{th} order. The value of q ranges from 0 and 1. the value of the fading parameter q shows the severity level of fading. $q=0$ represents the highest severity that can be modeled by Hoyt distribution and $q=1$ represents the lowest. The difference of Hoyt fading from Rayleigh fading is that it considers unequal powers in in-phase and quadrature phase components of the received signal.

Simulations are done for conventional SUCRe protocol considering the Hoyt fading channel. Fig. 8 shows the probability of resolving collision as a function of number of BS antennas for Hoyt fading channel model. Fig. 8(a) neglects the inter-cell interference (i.e. the adjacent cells are silent in RA block), while Fig. 8(b) considers the interference.

From fig.8, it can be clearly said that this scheme performs better in severe fading cases. with increasing values of q . This happens because the path-loss differences are lower in lower fading cases, which makes it hard to decide which UE has the strongest gain.



(a) Without interference from adjacent cells



(b) With interference from adjacent cells

Figure 8: SUCRe protocol performance over Hoyt fading channel for different values of q . (a) without interference case (b) with interference case

3) The Rician fading channel model

Earlier two models were suitable for modeling the fading distributions in a non-LOS environment. Rician fading is more suitable for the LOS scenario where the collection of multipath components contains a dominant component that has high strength as compared to other components. Rice

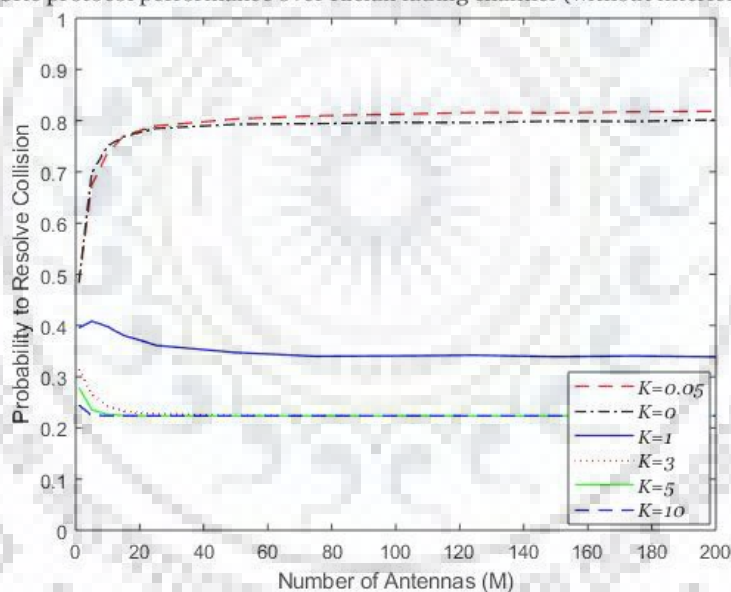
distribution is also known as Nakagami-n distribution. The PDF of rice distributed amplitude can be given by

$$p_X(x) = \frac{2(1+K)}{\Omega} x e^{-K - \frac{(1+K)x^2}{\Omega}} I_0\left(2x\sqrt{\frac{K(1+K)}{\Omega}}\right) \quad (31)$$

Where K is the rice factor. It is the fading parameter of rice distribution. K is defined as the ratio of the power of the dominant component to the total power of scattered component. Its value ranges from 0 to ∞ depending upon the environmental conditions.

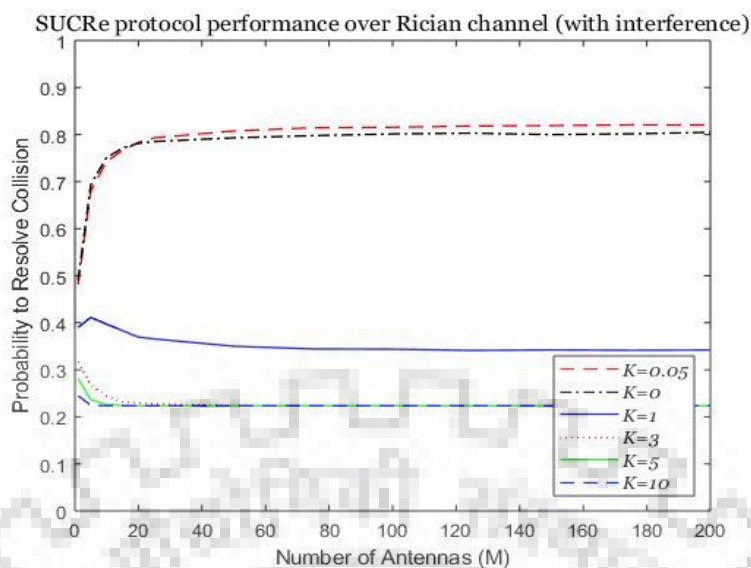
Simulations are done for conventional SUCRe protocol considering the Rician fading channel model. Fig. 9 shows the probability of resolving collision as a function of number of BS antennas over the Rician fading channel model for different value of fading parameter K . Fig. 9(a) neglects the inter-cell interference (i.e. the adjacent cells are silent in RA block), while Fig. 9(b) considers the interference.

SUCRe protocol performance over Rician fading channel (without interference)



(a) without interference from adjacent cells

Fig. 9 shows that as we increase the value of the fading parameter K (ratio of the power of dominant component to the total power of the scattered components), the performance deteriorates drastically, which is because of the fact that Rician channel is used for LoS cases, so the performance degrades as the path loss differences are lesser which makes the process of decision of a winning contender hard. Thus it is only suitable for the lower values of fading parameter.



(b) with interference from adjacent cells

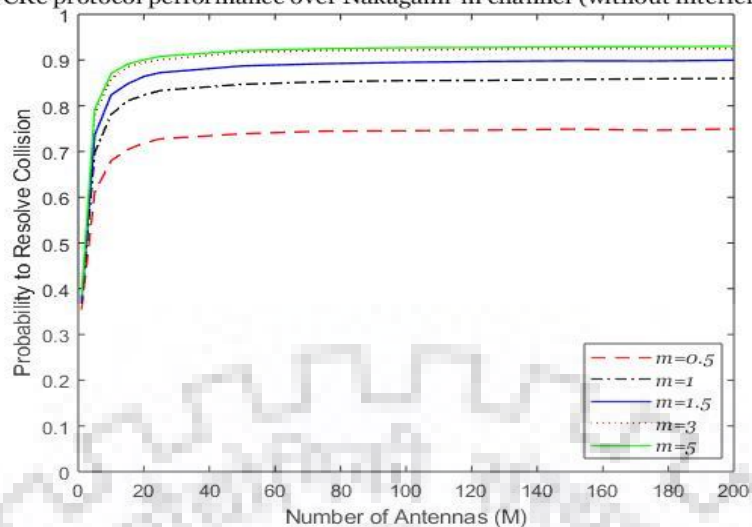
Figure 9: SUCRe protocol performance over the Rician fading channel with different Rician factors. (a) without interference from adjacent cells. (b) with interference from adjacent cells

4) Nakagami-m Fading channel model

Nakagami-m distribution is used to model fading scenario in various conditions (mostly in a non-LOS environment). Nakagami-m distribution is also commonly used to model the fading statistics of the received signal but it can model fading under generalized conditions up to a certain level. In the physical model, the fading parameter, m , is defined as the number of clusters of multipath components in the received signal.

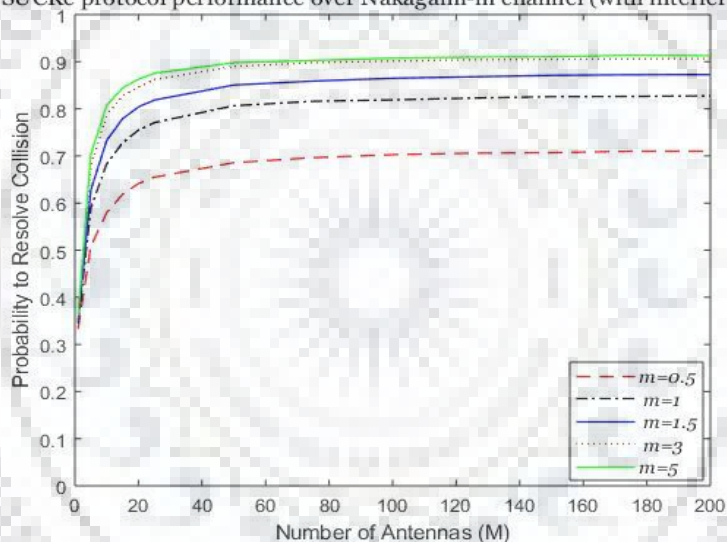
Simulations are done for conventional SUCRe protocol considering the Nakagami-m fading channel model. Fig. 10 shows the probability of resolving collision as a function of number of BS antennas over the Nakagami-m fading channel model for different value of fading parameter m . Fig. 10(a) neglects the inter-cell interference (i.e. the adjacent cells are silent in RA block), while Fig. 10(b) considers the interference. Here as the number of multipath clusters m increases, the probability of resolving collisions also increases.

SUCRe protocol performance over Nakagami-m channel (without interference)



(a) without inter-cell interference

SUCRe protocol performance over Nakagami-m channel (with interference)



(b) with inter-cell interference

Figure 10: SUCRe protocol performance over nakagami-m channels for different values of fading parameter m . (a) without inter-cell interference (b) with inter-cell interference

5) $\eta - \mu$ fading channel model

$\eta - \mu$ distribution is also suitable to model non-LOS environments. Like Nakagami-m fading, $\eta - \mu$ distribution also models a generalized fading scenario which includes the non-homogeneous environment which is composed of the reflecting obstacles, scattering elements, etc., of different physical properties. The physical model relates a number of clusters to the fading parameter, μ . Thus, this technique is valid for the generation of fading coefficients with discrete values of μ . The restriction is that the values of μ have to be half-integer, i.e., integer values of 2μ . For other values of μ , it is not possible to generate the channel coefficients using a simple set of instructions. It has two formats of

fading distribution. Format 1 is best for modeling suburban and rural areas undergoing a non-isotropic scattering environment. In non-isotropic scattering structure, the BS is assumed to be fixed with no scatterers around it whereas the UE is considered to be a moving unit and scatterers are distributed randomly around it. The format 2 approximates the fading conditions in urban areas undergoing isotropic scattering environment efficiently. In isotropic scattering structure, the BS is considered to be a fixed unit with no scatterers around it and UE is assumed to be a moving unit with uniformly distributed scatterers around it. As here, the crowded urban case is considered, format 2 will be taken into consideration [34].

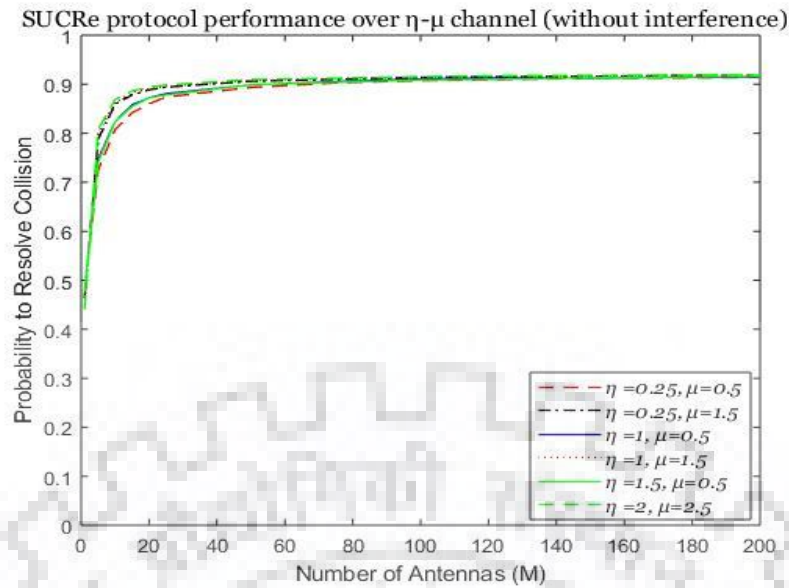
Due to the isotropic scattering structure in format 2, the signal arrives at receiver with the same phase thus the in-phase and the quadrature – phase components of the faded signal have identical powers. Hence the correlation coefficient ‘ η ’ is calculated between the in-phase and the quadrature phase component of the received signal. The PDF of $\eta - \mu$ distribution format 2 is given by [34]

$$f_P(\rho) = \frac{4\sqrt{\pi}\mu^{\mu+\frac{1}{2}}\rho^{2\mu}}{\eta^{\mu-\frac{1}{2}}\sqrt{1-\eta^2}\Gamma(\mu)} \exp\left[-\frac{2\mu\rho^2}{1-\eta^2}\right] \times I_{\mu-\frac{1}{2}}\left[\frac{2\eta\mu\rho^2}{1-\eta^2}\right], \quad (32)$$

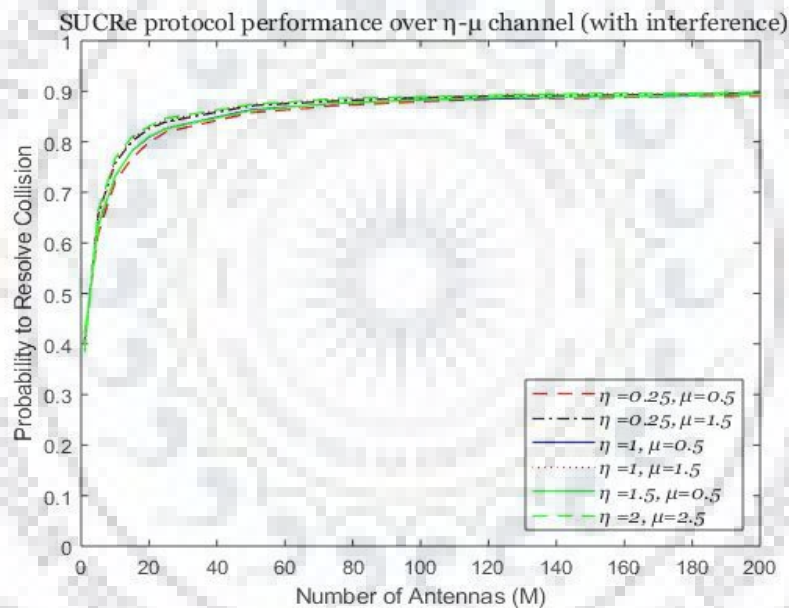
where $-1 < \eta < 1$ denotes the correlation coefficient between the in-phase and quadrature components of each multipath cluster, μ denotes the number of multipath clusters and ρ denotes the normalized envelope.

Simulations are done for conventional SUCRe protocol considering the $\eta - \mu$ fading channel model. Fig. 11 shows the probability of resolving collision as a function of number of BS antennas over the $\eta - \mu$ fading channel model for different value of η and μ . Fig. 11(a) neglects the inter-cell interference (i.e. the adjacent cells are silent in RA block), while Fig. 11(b) considers the interference.

As the number of the multipath cluster increases the amplitude of the received signal is also increased. This suggests that the severity of fading is decreased as the number of multipath clusters (μ) increases in a fading environment for a fixed value of η . Whereas for fixed μ and varying η , the incoming signal arrives with the same phase at receiver side due to isotropic scattering environment of format 2 so the values are almost overlapped as the value of correlation coefficient between in-phase and a quadrature component (η) of the received signal increases.



(a) without inter-cell interference



(b) with inter-cell interference

Figure 81: SUCRe protocol performance over η - μ channel for different values of η and μ . (a) without inter-cell interference (b) with inter-cell interference

6) κ - μ fading channel model

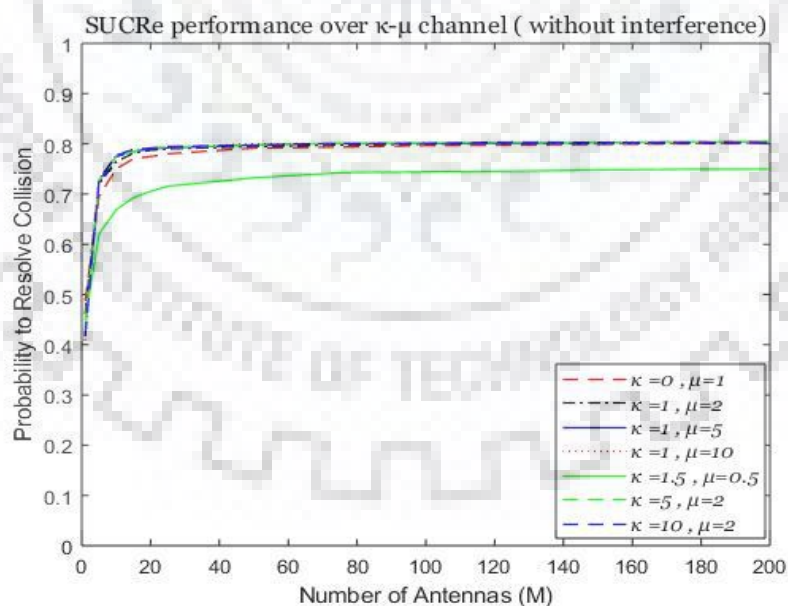
The proposal of κ - μ fading was laid down by M. D. Yacoub as a generalized distribution to model fading environment. Unlike Nakagami- m and η - μ fading models, κ - μ distribution is suitable to model LOS environments. Like Nakagami- m fading and η - μ distributions, κ - μ distribution also can model a generalized fading scenario which includes the non-homogeneous environment which is composed of the reflecting obstacles, scattering elements, etc. of different physical properties. The

physical model relates a number of clusters to the fading parameter, μ . Thus, this technique is valid for the generation of fading coefficients with discrete values of μ . The restriction is that the values of μ have to be integers. For other values of μ , it is not possible to generate the channel coefficients using a simple set of instructions. The PDF of $\kappa - \mu$ fading distribution is given by [39]

$$f_P(\rho) = \frac{2\mu \left(1 + \kappa^{\frac{\mu+1}{2}}\right)}{\kappa^{\frac{\mu-1}{2}} \exp(\mu\kappa)} \rho^\mu \exp[-\mu(1+\kappa)\rho^2] I_{\mu-1} \left[2\mu\sqrt{\kappa(1+\kappa)}\rho\right] \quad (33)$$

where P is the normalized fading envelope, $\kappa > 0$ is the ratio between the total power of dominant components and total power of scattered components and $I_\nu(\cdot)$ is the modified Bessel function of first kind and of order ν .

Simulations are done for conventional SUCRe protocol considering the $\kappa - \mu$ fading channel model. Fig. 12 shows the probability of resolving collision as a function of number of BS antennas over the $\kappa - \mu$ fading channel model for different value of κ and μ . Fig. 12(a) neglects the inter-cell interference (i.e. the adjacent cells are silent in RA block), while Fig. 12(b) considers the interference. It is clear from Fig. 12 that performance is better for lower values of fading parameter.



(a) without inter-cell interference

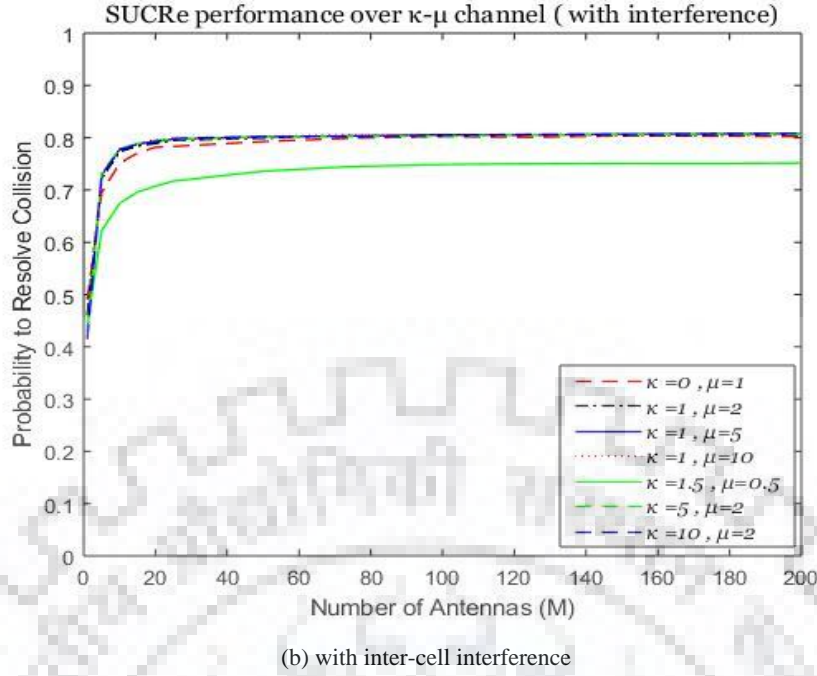


Figure 12: SUCRe protocol performance over the κ - μ channel for different value of κ and μ . (a) without inter-cell interference (b) with inter-cell interference

7) α - μ fading channel model

The proposal of α - μ distribution had been made with the name of Stacy distribution as a generalization to Gamma distribution. The initial proposal of Stacy distribution was to deal with the statistical problems, which was renamed later by M. D. Yacoub as α - μ distribution. α - μ distribution can be used to model fading channels in the environment characterized by non-homogeneous obstacles that may be nonlinear in nature. Like the other generalized fading models discussed earlier in this section, α - μ fading can also model various fading distributions as a special case. The PDF of α - μ fading distribution is given by [40]

$$f_P(\rho) = \frac{\alpha \mu^\mu \rho^{\alpha\mu-1}}{\Gamma(\mu) \exp(\mu \rho^\alpha)} \quad (34)$$

where P denotes the normalized envelope of fading signal, $\alpha > 0$ is an arbitrary parameter, $\mu > 0$ is the inverse of the normalized variance of P^α i.e. $\mu = \frac{E^2(P^\alpha)}{V(P^\alpha)}$ and $\Gamma(z) = \int_0^\infty t^{z-1} \exp(-t) dt$ is the Gamma function. Simulations are done for conventional SUCRe protocol considering the α - μ fading channel model. Fig. 13 shows the probability of resolving collision as a function of number of BS antennas over the α - μ fading channel model for different value of α and μ . Fig. 13(a) neglects the inter-cell interference (i.e. the adjacent cells are silent in RA block), while Fig. 13(b) considers the interference. From Fig. 13, it can be seen that, as fading parameter μ increases, which is associated with

the multipath clustering, the amount of fading decreases and thus the probability of resolving collisions increases

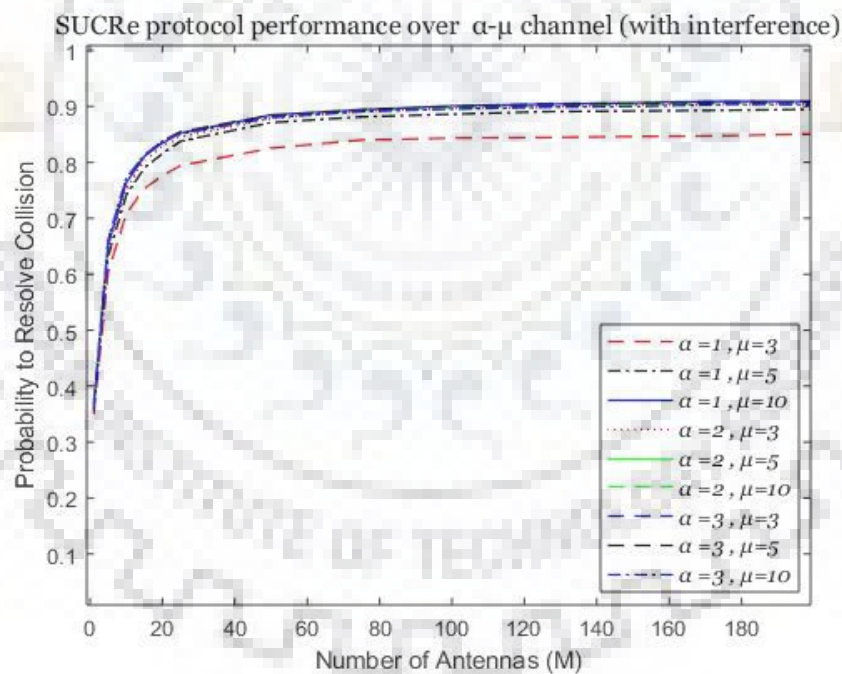
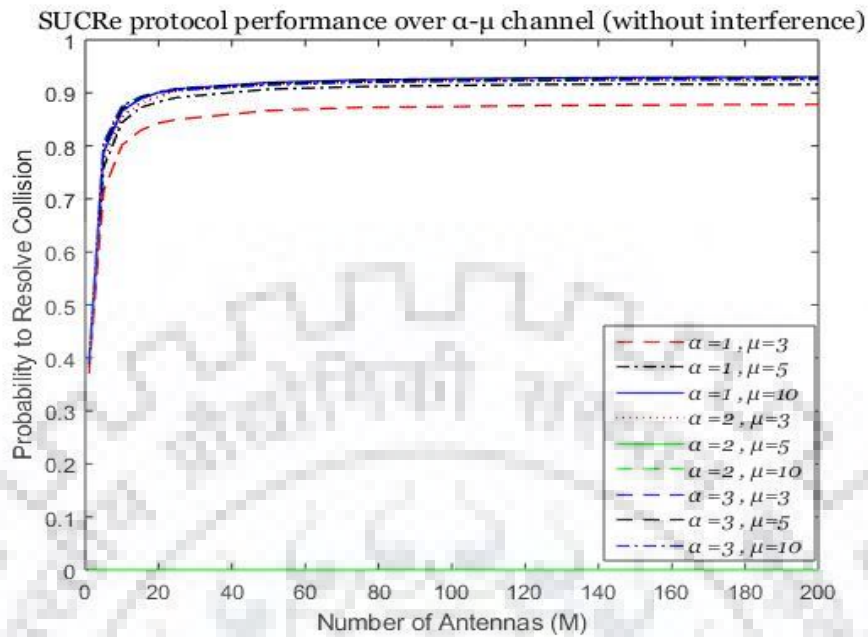


Figure 13: SUCRe protocol performance over $\alpha - \mu$ channel for different value of α and μ . (a) without inter-cell interference (b) with inter-cell interference

Table 2: Different fading channels and their properties

Fading channel	Environment	Fading Parameter	Special Cases
Rayleigh	Non- LOS	-	-
Hoyt / Nakagami-q	Non-LOS	q (Range: 0 to 1)	$q=0$: one-sided Gaussian $q=1$: rayleigh
Rician / Nakagami-n	LOS	K (Range:0 to ∞)	$K=0$: Rayleigh $K=\infty$: No fading
Nakagami-m	Non-LOS	m (Range:1 to ∞)	$m=1$: Rayleigh $m=0.5$: one-sided Gaussian $m>$: (approx.. rician) $m=\infty$: no fading
$\eta - \mu$	Non-LOS	η, μ (μ must be a half integer)	$\eta = 1, \mu = 0.5$: Rayleigh $\eta = 1, \mu = 0.25$: one-sided Gaussian $\eta = 1, \mu = 1.5$: nakagami-m $\eta = 0.25, \mu = 0.5$: hoyt
$\kappa - \mu$	LOS	κ, μ (μ must be an integer)	$\kappa = 0, \mu = 0.5$: one-sided Gaussian $\kappa = 0, \mu = 1$: Rayleigh $\kappa = 0, \mu = m$: nakagami-m $\kappa = K, \mu = 1$: rician
$\alpha - \mu$	Non-LOS	α, μ (μ must be an integer)	$\alpha = 2, \mu = m$: nakagami-m $\alpha = 2, \mu = 1$: Rayleigh $\alpha = 2, \mu = 0.5$: one-sided Gaussian $\alpha = 1, \mu = 1$: exponential

5.2 Probability of resolving collisions by SUCRe protocol

The parameters chosen for the calculation of the probability of resolving collisions by SUCRe protocol are summarized in the table below:

Table 3: Simulation parameters for the evaluation of the probability of resolving collisions

Parameter	Value
hard decision rule	-
Probability of UE being active	$P_a = 0.1 \%$

Length of the training sequence	$\tau_p = 10$
Number of inactive devices	$K_0 = 5000$
The radius of each hexagon d_{\max}	250m
Min. distance between two UEs d_{\min}	25m
\bar{d}	$10^{-3.53}$
Path loss exponent	3.8
Shadowing standard deviation	8 dB
Probability of accessing the network by each UE	0.5 %

The probability to resolve collisions is defined as

$$\begin{aligned}
 P_{\text{resolved}} &= \mathbb{E}\{P_{|\mathcal{S}_t|, \text{resolved}} \mid |\mathcal{S}_t| \geq 1\} \\
 &= \sum_{N=1}^{K_0} \frac{P_{N, \text{resolved}} \binom{K_0}{N} \left(\frac{P_a}{\tau_p}\right)^N \left(1 - \frac{P_a}{\tau_p}\right)^{K_0-N}}{1 - \left(1 - \frac{P_a}{\tau_p}\right)^{K_0}}, \quad (35)
 \end{aligned}$$

Comparison of SUCRe protocol over different channels(without interference)

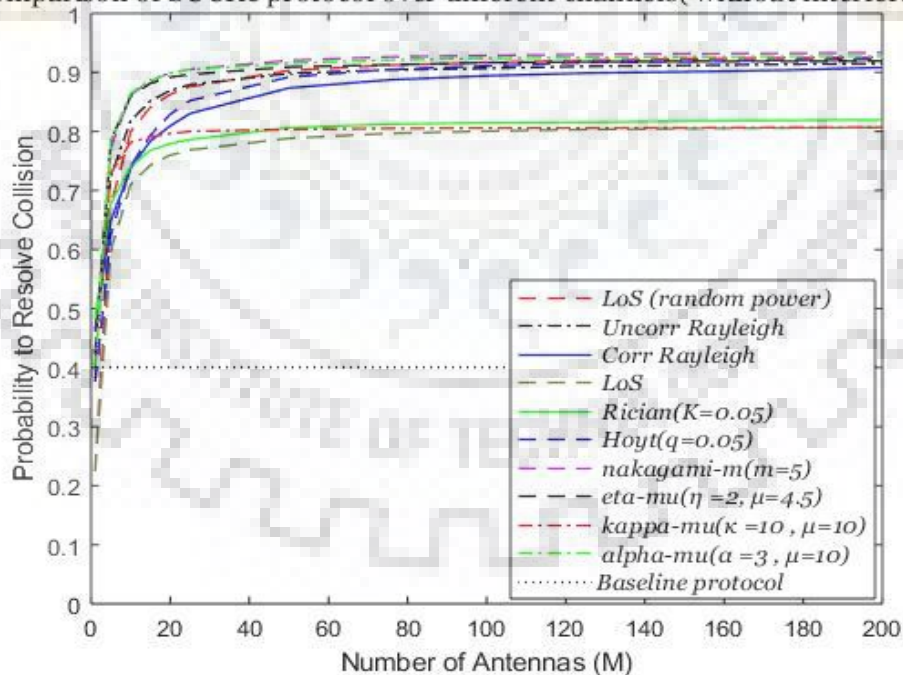


Figure 14(a): without interference from other cells

Fig. 14 shows the SUCRe protocol performance in terms of probability of resolving collisions as the function of number of antennas in the BS for the fading models that are discussed above. It can be

directly observed the probability of resolving collisions increases as number of BS antennas increases, thus it can be inferred that SUCRe protocol depends on the channel hardening and Favourable propagation characteristics of the massive MIMO channels.

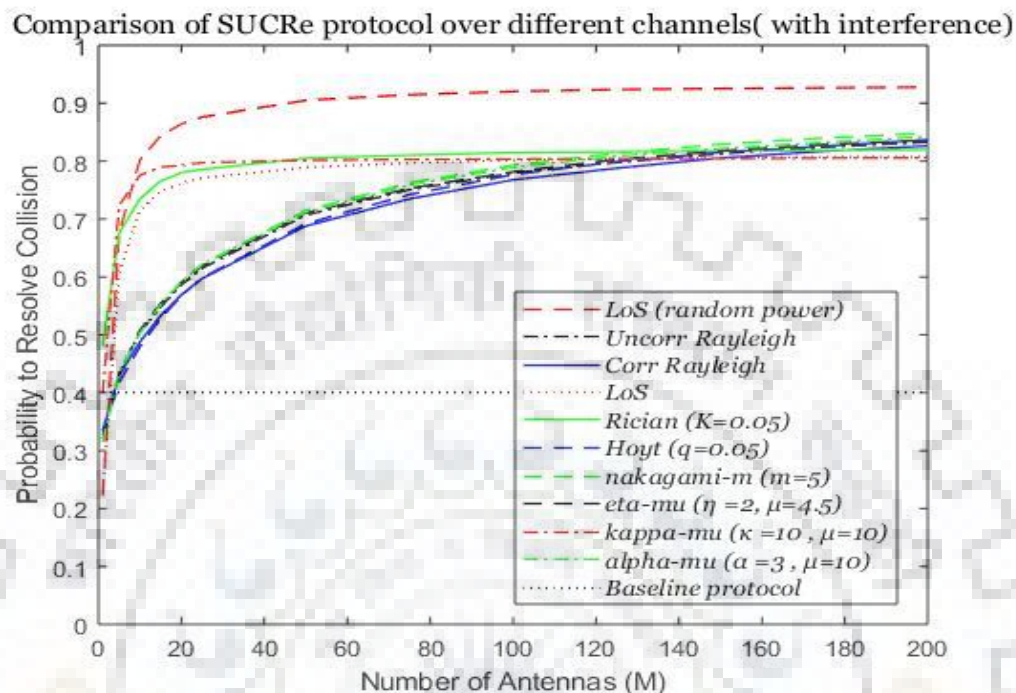


Figure 14(b): with interference from other cells

Figure 14: Probability of resolving collisions, as a function of the number of BS antennas, in a highly loaded cellular network with or without inter-cell interference

Uncorrelated Rayleigh performs better than correlated Rayleigh fading, but the difference is small when M is large. The LoS model has a bit worse performance because the conventional SUCRe protocol relies on the selection of the strongest user. However, in LoS case, the path loss differences are lower so it is hard to decide which UE has the strongest signal gain. Table 4 summarizes the performance for all the channels in both with interference and without interference cases terms of collision resolution capability in % for different values of M (10, 50, 100, 200). The fading parameter values for Rician, Hoyt, nakagami-m, etc. channels are chosen based on fig. 13, 14, 15,16,17,18 (the best case scenarios). The baseline protocol is the simple case, where, if a collision happens, the process ends there abruptly and the pilots are retransmitted in the coming random access slots. Fig. 14 also depicts that the conventional SUCRe protocol is able to admit roughly four times as many UEs per RA pilot than the baseline scheme. There is only a slight performance degradation in interference cases which suggests that SUCRe protocol performs well for interference as well as without interference cases.

Table 4: comparison of SUCRe protocol over different fading channels

Fading channels	collisions resolved for M=10 (%)		collisions resolved for M=50 (%)		collisions resolved for M=100 (%)		collisions resolved for M=200 (%)	
	Without intf.	With intf.	Without intf.	With intf.	Without intf.	With intf.	Without intf.	With intf.
LoS with random power back off	79.96	80.2	90.31	90.5	91.65	92.04	92.56	92.77
Uncorrelated Rayleigh fading	81.78	50.27	89.81	70.67	90.69	77.94	91.52	83.29
Correlated Rayleigh fading	74.11	47.97	87.36	68.78	89.42	76.76	90.82	82.61
LoS	71.03	71.57	78.84	78.91	80.05	80.17	80.71	80.75
Rician	74.02	73.47	80.62	80.51	81.47	81.48	81.97	81.96
Hoyt	74.11	47.97	89.21	69.21	91.08	77.67	92.22	83.90
Nakagami-m	86.52	50.27	92.03	71.48	92.86	79.31	93.35	84.82
η - μ	86.52	50.27	90.92	71.06	91.65	78.16	91.93	82.53
κ - μ	78.15	77.54	80.35	80.13	80.58	80.36	80.71	80.58
α - μ	86.52	50.27	91.56	71.18	92.39	78.9	92.74	84.23
Baseline protocol	40.08	40.08	40.08	40.08	40.08	40.08	40.08	40.08

5.3 Tuning Probabilities Using Bias Terms

Now, using (21) and (23) from chapter 3, simulations are done to observe the effect of the bias term ϵ_k on the decisions. This is done by choosing a value of ϵ_k corresponds to adding δ standard deviations of $\|\mathbf{h}_k\|^2/M$ around its mean value β_k). These simulations have been performed for a simple uncorrelated Rayleigh fading channel. Fig. 15 shows the probabilities of resolving collision,

false positive and false negative as a function of δ , for $M=100$. These simulations are also done for both with and without interference cases.

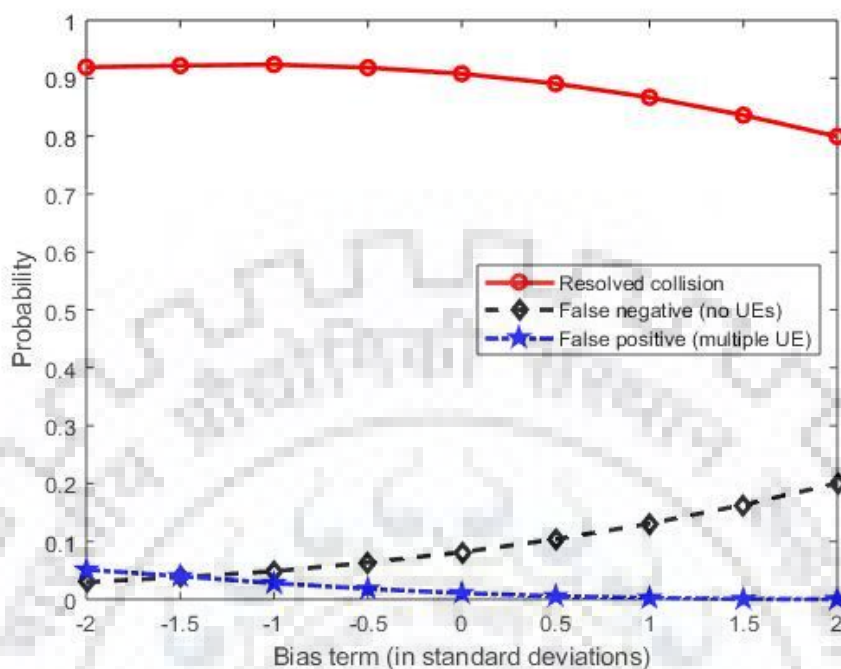


Figure 15(a): without interference

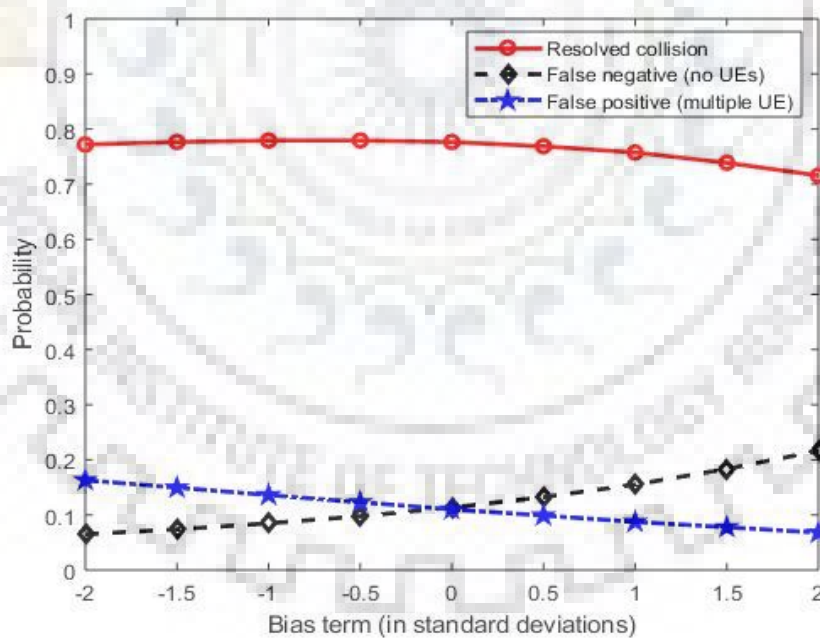


Figure 15(b): with interference case

Figure 15: for different bias terms in the hard decision rule, the probability of resolving collisions, false negatives, and false positives are illustrated

UE k can be encouraged to assign itself the contention winner by subtracting one or two δ from $\hat{\alpha}_{t,k}/2$ in the decision rule,. This results in a higher probability of resolving collisions, at the cost of more false positives where more than one UEs try to retransmit their pilot sequence in the third step. In

contrast, by adding one or two standard deviations to $\hat{\alpha}_{t,k}/2$ in the decision rule, UE k can be discouraged from assigning itself the winner of the contention and thereby the probability of false positives reduces to zero—at the cost of resolving fewer collisions and having more false negatives implying that no UE will be retransmitting its pilot in the third step.

5.4 Probability of Failed Attempts & Average Number of Random Access Attempts

Whenever any UE that is trying to access the wireless network, experiences a collision which could not be resolved by RA protocol, then that UE will be attempting for the access again after waiting for the random amount of time. However, after making 10 access attempts, the UE stops the retransmission considering that access has been denied by the network. This is the same baseline protocol chosen for simulation in Fig. 14, only with a slight modification of 10 access attempts before ending the process and then trying in next random access slot. The evaluation of the average number of RA attempts and the probability of failed transmission is done for SUCRe protocol [35] and the proposed SUCRe using the soft decision rule. The simulation parameters taken to determine the same are described in table 5.

Table 5 Simulation parameters for evaluation of the average number of access attempts and the probability of failed attempts

Parameter	Value
Soft decision rule	Sigmoid function
Probability of UE being active	$P_a = 0.1 \%$
Length of the training sequence	$\tau_p = 10$
Number of inactive devices	$K_0 \in [1; 16000]$
The radius of each hexagon d_{\max}	250m
Min. distance between two UEs d_{\min}	25m
\bar{d}	$10^{-3.53}$
Path loss exponent	3.8
Shadowing standard deviation	8 dB

Fig. 16 (a) shows the average number of access attempts as the function of number of inactive UEs and Fig. 16(b) shows the probability of failed access attempts as the function of number of inactive UEs for both conventional SUCRe and the SUCRe incorporating soft decision rule for without and with interference (from adjacent cells) cases. one can clearly see that a lesser number of RA attempts are required in soft SUCRe as compared to conventional SUCRe. The performance comparison of soft SUCRe with conventional SUCRe has been done and summarized in table 6.

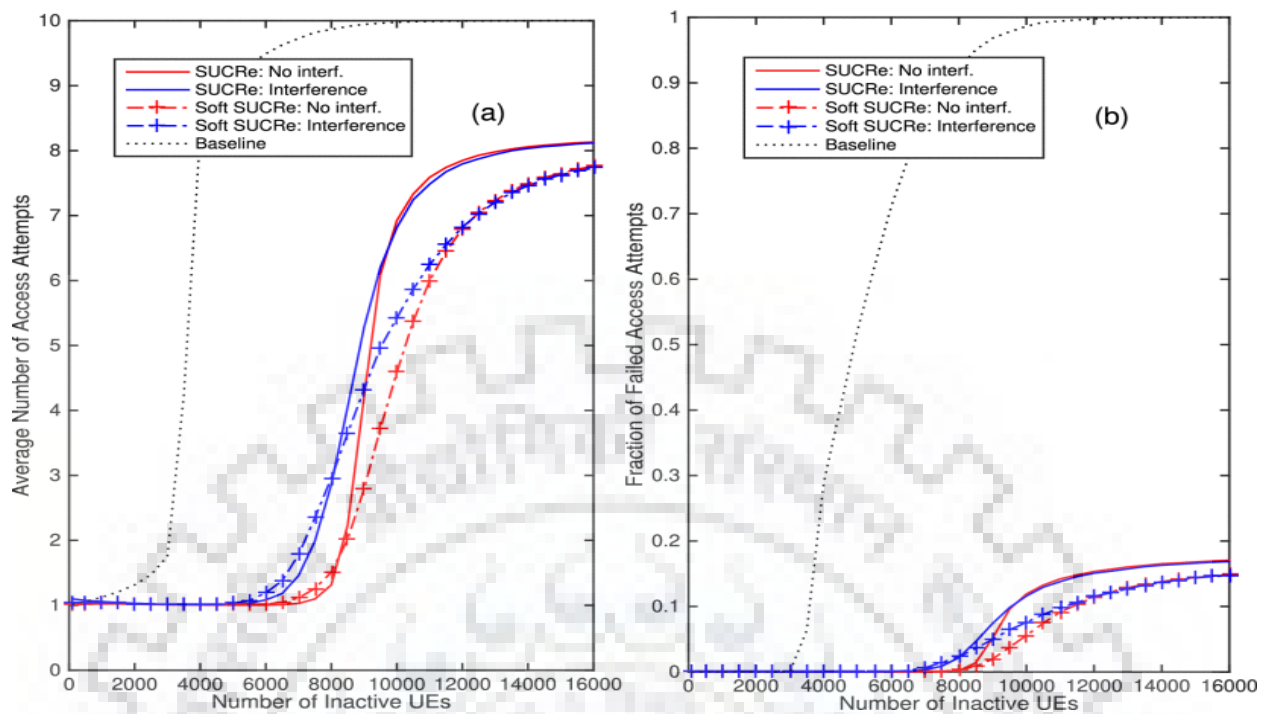


Figure 16: RA performance in a crowded urban scenario. (a) The average number of RA attempts for SUCRe and soft SUCRe. (b) Probability of failed attempts

Table 6: Reduction in the average number of RA attempts and increment of active UEs in soft SUCRe in comparison with conventional SUCRe

Metric	Interference	K_0					
		8000	9000	10000	12000	16000	20000
Reduction in RA attempts	without	-0.196	1.414	2.336	1.049	0.372	0.294
	with	-0.100	0.955	1.392	0.385	0.384	0.266
Increment in active UEs	without	-0.0073	0.289	0.6327	0.473	0.350	0.349
	with	-0.0104	0.219	0.4224	0.422	0.341	0.329

It shows the reduction in an average number of RA attempts of the soft SUCRe protocol in comparison with conventional SUCRe, with and without interference from adjacent cells. It also depicts the additional active UEs that can be admitted in soft SUCRe. The performance is slightly worse when the number of UEs is less than 8500, which is correct as soft SUCRe works well for a high number of contentions and the low disparity between their fading coefficients.

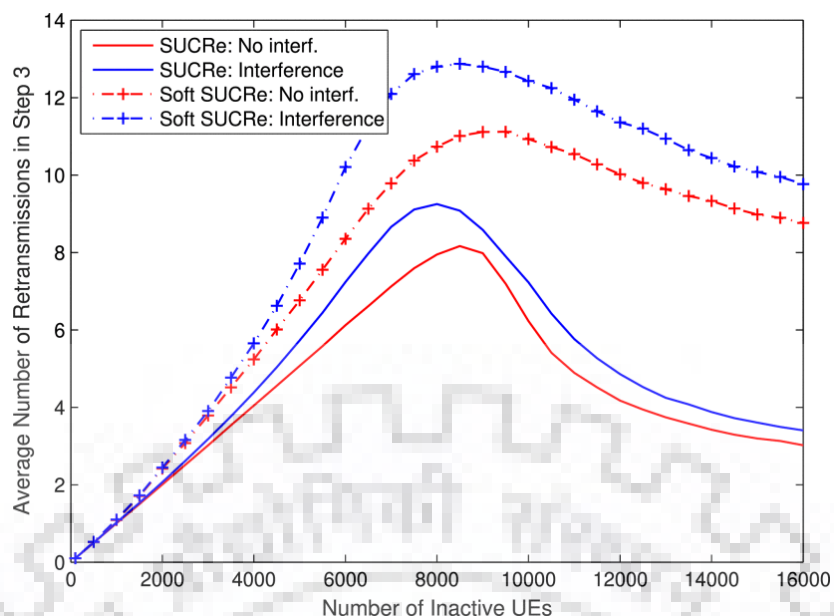


Figure 17: average number of pilot retransmission

Fig. 17 depicts the average number of pilot retransmission in step 3 for a number of inactive UEs ranging from [0,16000] conventional SUCRe protocol and its modified version. For conventional SUCRe, the curve has its peak approximately around 9000 UEs in without interference case and around 8000 UEs for with interference case [35]. Initially, the number of retransmissions increases because of an increasing number of accessing UEs, but after a certain threshold, the number of collisions becomes very high and the hard decision rule in (21) is rarely satisfied so the average number of retransmissions done in the third step decreases after that threshold point. However, soft SUCRe protocol mitigates this degradation in an average number of pilot retransmission which in turn results in an improvement in overall RA performance.

Chapter 6

Conclusions and Future Scope

This work is primarily focused on RA in crowded massive MIMO networks. The simulations result depicted that the conventional SUCRe protocol is capable to resolve around 92-93% collisions and it works well in the presence of inter-cell interference and also performs satisfactorily for any choice of channel distribution. In overloaded situations, where more UEs request pilots than there are RA resources, SUCRe protocol does not fail and continues to admit a subset of the accessing UEs. When the comparative analysis is done on a number of channels with different distribution and fading parameter, it is seen that it performs well with most of them. Its performance has been further improved by proposing a new decision rule “soft decision rule” which is based on sigmoid function. It reduces the number of average RA attempts and probability of failed access attempts marginally as compared to conventional SUCRe where hard decision rule is used.

Some new protocols have also been proposed over time. one of them is SUCR-TA (SUCR incorporated with timing advance information) protocol which takes into account the propagation delay and picks an appropriate TA information for each pilot sequence which is activated by the UEs so that an overall number of contenders reduce in the subsequent steps.

Another one is the SUCR-IPA (SUCR combined idle pilot access) which allows the UEs that have failed to access the network according to SUCR, to contend for the idle pilots again in the same random access slots. It reduces the number of access attempts significantly.

We can combine all the three proposed protocols SUCR-TA-IPA which will have advantages of all of the three protocols thus it will have outstanding performance in improving system throughput thereby reducing the number of access attempts significantly. Also, the soft decision rule can be adopted in the hybrid SUCR-TA-IPA protocol to further improve the performance.

Bibliography

- [1] "Ericsson mobility report", Stockholm, Sweden, Tech. Report, Nov. 2015, available: <http://www.ericsson.com/res/docs/2015/mobility-report/ericsson-mobility-report-nov-2015.pdf>.
- [2] M. Fallgren, B. Timus, D1.1: Scenarios Requirements and KPIs for 5G Mobile and Wireless System, 2013.
- [3] F. Boccardi, R. W. Heath, A. Lozano, T. L. Marzetta, P. Popovski, "Five disruptive technology directions for 5G", *IEEE Commun. Mag.*, vol. 52, no. 2, pp. 74-80, Feb. 2014.
- [4] T. L. Marzetta, "Noncooperative cellular wireless with unlimited numbers of base station antennas", *IEEE Trans. Wireless Commun.*, vol. 9, no. 11, pp. 3590-3600, Nov. 2010.
- [5] E. Björnson, E. G. Larsson, M. Debbah, "Massive MIMO for maximal spectral efficiency: How many users and pilots should be allocated?", *IEEE Trans. Wireless Commun.*, vol. 15, no. 2, pp. 1293-1308, Feb. 2016.
- [6] E. Björnson, E. G. Larsson, T. L. Marzetta, "Massive MIMO: Ten myths and one critical question", *IEEE Commun. Mag.*, vol. 54, no. 2, pp. 114-123, Feb. 2016.
- [7] J. Vieira et al., "A flexible 100-antenna testbed for massive MIMO", *Proc. IEEE Globecom Workshop Massive (MIMO)*, pp. 287-293, Dec. 2014.
- [8] J. Jose, A. Ashikhmin, T. L. Marzetta, S. Vishwanath, "Pilot contamination and precoding in multi-cell TDD systems", *IEEE Trans. Wireless Commun.*, vol. 10, no. 8, pp. 2640-2651, Aug. 2011.
- [9] H. Huh, G. Caire, H. C. Papadopoulos, S. A. Ramprasad, "Achieving 'massive MIMO' spectral efficiency with a not-so-large number of antennas", *IEEE Trans. Wireless Commun.*, vol. 11, no. 9, pp. 3226-3239, Sep. 2012.
- [10] J. Hoydis, S. ten Brink, M. Debbah, "Massive MIMO in the UL/DL of cellular networks: How many antennas do I need?", *IEEE J. Sel. Areas Commun.*, vol. 31, no. 2, pp. 160-171, Feb. 2013.
- [11] H. Q. Ngo, E. G. Larsson, T. L. Marzetta, "Energy and spectral efficiency of very large multiuser MIMO systems", *IEEE Trans. Commun.*, vol. 61, no. 4, pp. 1436-1449, Apr. 2013.

-
- [12] H. Yin, D. Gesbert, M. Filippou, Y. Liu, "A coordinated approach to channel estimation in large-scale multiple-antenna systems", *IEEE J. Sel. Areas Commun.*, vol. 31, no. 2, pp. 264-273, Feb. 2013.
- [13] A. Adhikary, J. Nam, J. Y. Ahn, G. Caire, "Joint spatial division and multiplexing—The large-scale array regime", *IEEE Trans. Inf. Theory*, vol. 59, no. 10, pp. 6441-6463, Oct. 2013.
- [14] E. Björnson, J. Hoydis, M. Kountouris, M. Debbah, "Massive MIMO systems with non-ideal hardware: Energy efficiency estimation and capacity limits", *IEEE Trans. Inf. Theory*, vol. 60, no. 11, pp. 7112-7139, Nov. 2014.
- [15] L. Lu, G. Y. Li, A. L. Swindlehurst, A. Ashikhmin, R. Zhang, "An overview of massive MIMO: Benefits and challenges", *IEEE J. Sel. Topics Signal Process.*, vol. 8, no. 5, pp. 742-758, Oct. 2014.
- [16] E. Björnson, E. G. Larsson, "Three practical aspects of massive MIMO: Intermittent user activity pilot synchronism and asymmetric deployment", *Proc. IEEE GLOBECOM Workshops*, pp. 1-6, Dec. 2015.
- [17] M. Hasan, E. Hossain, D. Niyato, "Random access for machine-to-machine communication in LTE-advanced networks: Issues and approaches", *IEEE Commun. Mag.*, vol. 51, no. 6, pp. 86-93, Jun. 2013.
- [18] N. K. Pratas, H. Thomsen, C. Stefanovic, P. Popovski, "Code-expanded random access for machine-type communications", *Proc. IEEE GLOBECOM Workshops*, pp. 1681-1686, Sep.
- [19] J. H. Sørensen, E. de Carvalho, P. Popovski, "Massive MIMO for crowd scenarios: A solution based on random access", *Proc. IEEE GLOBECOM Workshops*, pp. 352-357, Jun. 2014
- [20] E. de Carvalho, E. Björnson, E. G. Larsson, P. Popovski, "Random access for massive MIMO systems with intra-cell pilot contamination", *Proc. IEEE ICASSP*, pp. 3361-3365, Mar. 2016
- [21] L. Sanguinetti, A. A. D'Amico, M. Morelli, M. Debbah, "Random access in uplink massive MIMO systems: How to exploit asynchronicity and excess antennas", *Proc. IEEE GLOBECOM*, pp. 1-5, May 2016.
- [22] E. Paolini, G. Liva, M. Chiani, "High throughput random access via codes on graphs: Coded slotted ALOHA", *Proc. IEEE Int. Conf. Commun. (ICC)*, pp. 1-6, Sep. 2011.
- [23] E. Paolini, C. Stefanovic, G. Liva, P. Popovski, "Coded random access: How coding theory helps to build random access protocols", *IEEE Commun. Mag.*, vol. 53, no. 6, pp. 144-150,

- Jun. 2015.
- [24] E. Björnson, E. de Carvalho, E. G. Larsson, P. Popovski, "Random access protocol for massive MIMO: Strongest-user collision resolution (SUCR)", Proc. IEEE ICC, pp. 1-6, May 2016.
- [25] H. Ngo, E. Larsson, T. Marzetta, "Aspects of favorable propagation in massive MIMO", Proc. EUSIPCO, pp. 76-80, Sep. 2014.
- [26] R. Couillet, M. Debbah, Random Matrix Methods for Wireless Communications, Cambridge, U.K.:Cambridge Univ. Press, 2011.
- [27] S. L. Loyka, "Channel capacity of MIMO architecture using the exponential correlation matrix", IEEE Commun. Lett., vol. 5, no. 9, pp. 369-371, Sep. 2001.
- [28] Spatial Channel Model for Multiple Input Multiple Output (MIMO) Simulations (Release 13), Dec. 2015.
- [29] J. Capetanakis, "Tree algorithms for packet broadcast channels", IEEE Trans. Inf. Theory, vol. IT-25, no. 5, pp. 505-515, Sep. 1979.
- [30] J. H. Sørensen, C. Stefanović, P. Popovski, "Coded splitting tree protocols", Proc. IEEE ISIT, pp. 2860-2864, Sep. 2013.
- [31] I. S. Gradshteyn, I. M. Ryzhik, Table of Integrals Series and Products, San Diego, CA, USA:Academic, 1980
- [32] S. M. Kay, Fundamentals of Statistical Signal Processing: Estimation Theory, Englewood Cliffs, NJ, USA:Prentice-Hall, 1993.
- [33] Brijesh Kumbhani, Rakshesh Singh Kshetrimayum - MIMO wireless communications over generalized fading channels (2017, CRC Press_Taylor & Francis)
- [34] C.Priyanka and V.Nithya , "Physical Scenario Perusal of eta-mu Fading Channels" , IEEE 2015 International Conference on Communications and Signal Processing (ICCSP),Nov. 2015
- [35] E. Björnson, E. de Carvalho, J. H. Sørensen, E. G. Larsson, P. Popovski, "A random access protocol for pilot allocation in crowded massive MIMO systems", IEEE Trans. Wireless Commun., vol. 16, no. 4, pp. 2220-2234, Apr 2017.
- [36] M. Hochwald, T. L. Marzetta, and V. Tarokh, "Multiple-antenna channel hardening and its implications for rate feedback and scheduling," IEEE Transactions on Information Theory,

- vol. 50, no. 9, pp. 1893–1909, 2004.
- [37] E. Björnson, E. de Carvalho, J. H. Sørensen, E. G. Larsson, P. Popovski, “Random Access Protocols for Massive MIMO”, IEEE communications magazine, vol. 55, May 2017
- [38] O.Y. Bursalioglu et al. , “RRH based Massive MIMO with “on the Fly” pilot contamination control”, Proc. IEEE ICC, 2016
- [39] Michel Daoud Yacoub, “The $\kappa - \mu$ distribution and the $\eta - \mu$ distribution”, IEEE Antennas and Propagation Mag., vo. 49, June 2007
- [40] Michel Daoud Yacoub, “The $\alpha - \mu$ distribution: A physical fading model for the Stacy distribution”, IEEE Transactions on vehicular technology, vol. 56, Jan. 2007
- [41] Trinh Van Chien, E. Björnson, “Massive MIMO Communications” book



Thesis

ORIGINALITY REPORT



PRIMARY SOURCES

arxiv.org
Internet Source

6%

Jose Carlos Marinello Filho, Taufik Abrao.
"Collision Resolution Protocol via Soft Decision Retransmission Criterion", IEEE Transactions on Vehicular Technology, 2019

Publication

3%

Emil Bjornson, Elisabeth de Carvalho, Jesper H. Sorensen, Erik G. Larsson, Petar Popovski.
"A Random Access Protocol for Pilot Allocation in Crowded Massive MIMO Systems", IEEE Transactions on Wireless Communications, 2017

Publication

1%

Submitted to Indian Institute of Technology, Madras

Student Paper

1%

Elisabeth de Carvalho, Emil Bjornson, Jesper H. Sorensen, Petar Popovski, Erik G. Larsson.
"Random Access Protocols for Massive MIMO",

1%

IEEE Communications Magazine, 2017

Publication

Submitted to University of Stellenbosch, South Africa

1%

Student Paper

C. Priyanka, V. Nithya. "Physical scenario perusal of eta-mu fading channels", 2015 International Conference on Communications and Signal Processing (ICCSP), 2015

1%

Publication

Submitted to The University of Manchester

<1%

Student Paper

link.springer.com

<1%

Internet Source

Emil Bjornson, Elisabeth de Carvalho, Erik G. Larsson, Petar Popovski. "Random access protocol for massive MIMO: Strongest-user collision resolution (SUCR)", 2016 IEEE International Conference on Communications (ICC), 2016

<1%

Publication

Luca Sanguinetti, Antonio A. D'Amico, Michele Morelli, Merouane Debbah. "Random Access in Massive MIMO by Exploiting Timing Offsets and Excess Antennas", IEEE Transactions on Communications, 2018

<1%

Publication

Submitted to Jawaharlal Nehru Technological University

Student Paper

<1%

Suresh Kumar Balam, P. Siddaiah, Srinivas Nallagonda. "Throughput analysis of cooperative cognitive radio network over generalized κ - μ and η - μ fading channels", Wireless Networks, 2018

Publication

<1%

Nidhi Bhargav, Simon L. Cotton. "Secrecy capacity analysis for α - μ / κ - μ and κ - μ / α - μ fading scenarios", 2016 IEEE 27th Annual International Symposium on Personal, Indoor, and Mobile Radio Communications (PIMRC), 2016

Publication

<1%

www.thinkinglean.com

Internet Source

<1%

Exclude quotes On

Exclude matches < 20 words

Exclude bibliography On